Check for updates

ChemCatChem

Review
doi.org/10.1002/cctc.202400393

Chemistry Europe
European Chemical Societies Publishing

www.chemcatchem.org

Advances in the Homogeneously Catalyzed Hydrogen Production from Biomass Derived Feedstocks: A Review

Andrea Fasolini+,[a, b, c] Giulia Martelli+,[a, b] Andrea Piazzi,[a, b] Massimiliano Curcio,[a, b] Jacopo De Maron,[a, b, c] Francesco Basile,[a, b, c] and Rita Mazzoni*[a, b, c]

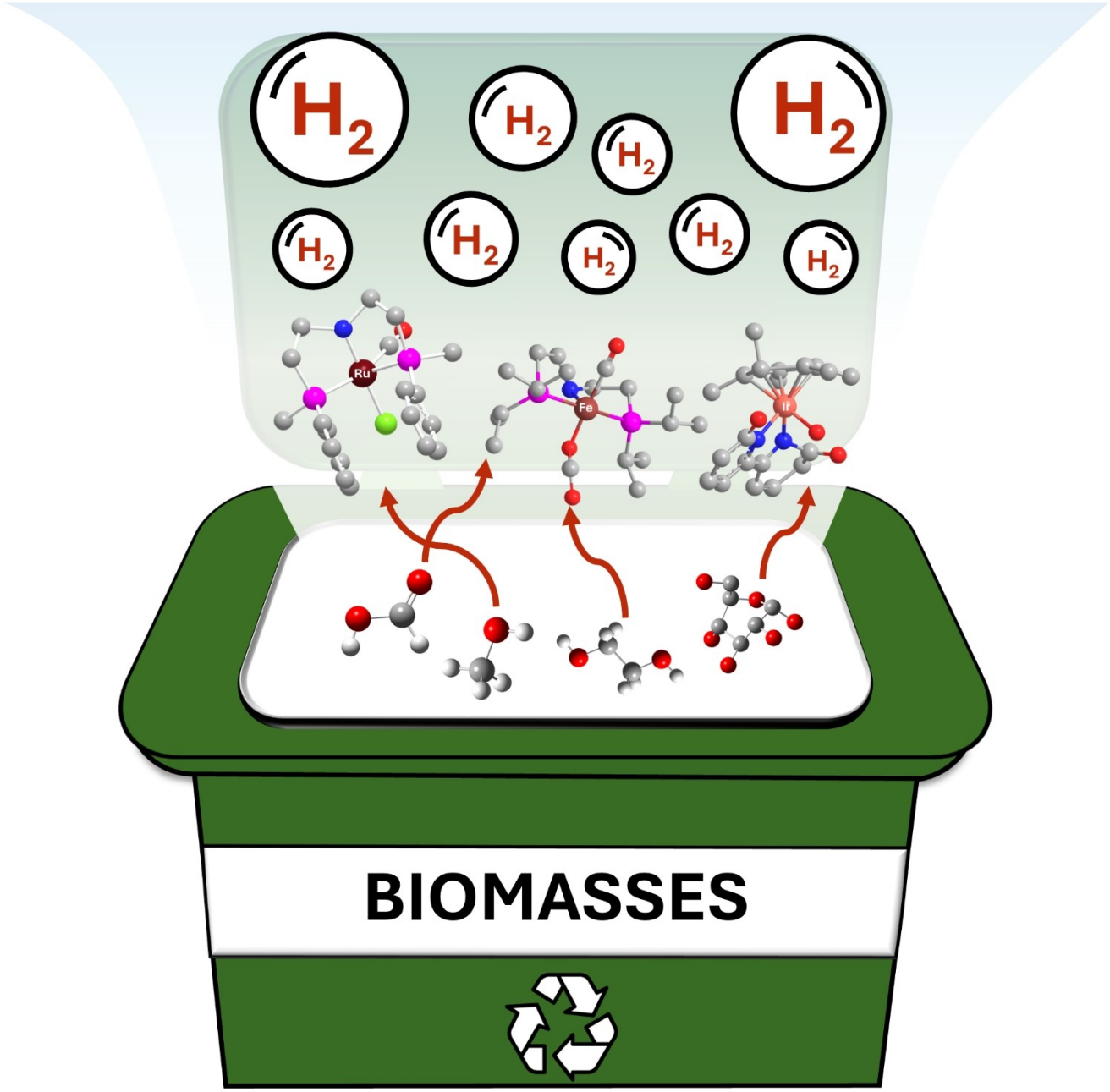

© 2024 The Author(s). ChemCatChem published by Wiley-VCH GmbH

Biomass–derived feedstocks for hydrogen production are crucial as an alternative to fossil fuel especially in those areas where green electricity and clean water are scarce. In this framework the transformation of simple (formic acid, alcohols) and more complex (polyalcohols, sugars and cellulose) bio–derivatives in pure hydrogen is recognized as a promising approach. Parallel to great effort in heterogeneous catalysis, milder molecular systems represent a more selective eye for alternative solutions and mechanistic insights. In the present review the introduction summarizes the challenges in the catalytic utilization of biomass–derived feedstocks, followed by the advances in homogeneously catalyzed hydrogen production from different substrates which will cover formic acid, with oustanding efficiency with noble metals and promising results with earth abundant ones and alcohols and polyalcohols, with particular emphasis to the development of heterogenized systems, ligand assisted catalysts and bi-catalytic synergistic solutions which allow to avoid base and to promote catalyst stability and recyclability. In the last part, description of hydrogen production from more complex substrates, such as sugars and cellulose, will show the role of molecular complexes in main and side reactions. Critical comments on the reported advances are provided along the whole discussion.

1. Hydrogen: A Secondary Energy of the Future

Hydrogen, a versatile energy vector, is one of the tools envisioning and unlocking a future not dependent by fossil fuels and with low or even negative carbon dioxide emissions. Traditionally hydrogen has been mainly produced from fossil fuels themselves (mainly by steam reforming of natural gas) and used in the chemical industry for ammonia production, petrol upgrading and hydrogenation reactions. However, the substitution of green hydrogen in these sectors and its employment as an energy carrier can help to deal with different energy challenges. Green hydrogen can lead the decarbonization of hard-to-abate sectors like aviation, shipping, chemicals, steel production. Being an option to store energy over time, hydrogen can also help the permeation of different renewables energy in the electricity system. However, developing a novel hydrogen value chain without a pre–existing structure is a great challenge of our time. For this reason, different initiatives have been carried out worldwide to boost the development and scale up of hydrogen technologies. In Europe, the European community hydrogen strategy together with REPowerEU has set the target of 10 million tonnes of produced and imported hydrogen by 2030.[1] Moreover, through Mission Innovation,[2] it has set the objective to reduce the hydrogen cost to make it competitive with fossil fuels. In this field, the US Department of Energy plans to reduce the cost of hydrogen from the actual 5 dollars per kg to just 1 dollar per kg in one decade.[3] In India, the National Green Hydrogen Mission aims at producing 5 Mt/y of renewable hydrogen by 2030.[4] China as well has launched a plan that aims at reaching a renewable hydrogen production of 1–2 Mt/y by 2025.[5] Overall, an investment up to 750 billion dollars will be involved for the development of the project announced through 2030.[6]

Although hydrogen production from electrolysers is paving the way to the growing hydrogen infrastructure, the development of alternative processes for hydrogen production is crucial to differentiate the feedstocks and operate in those areas where green electricity and clean water are scarce. In this framework the employment of biomass derived feedstocks can play an important role, because lignocellulosic biomasses, thanks to their high availability of multiple thousands of tons of dry material,[7] can be an alternative to fossil fuels. Three main components are found in lignocellulosic biomasses, namely lignin (around 20 wt.%), cellulose (around 45 wt.%) and hemicellulose (around 35 wt.%).[8] Although this adds complexity to the feedstock, two of these three components (cellulose and hemicellulose) can be converted into hydrogen or to molecules that are easily reformable to hydrogen itself. In this review the utilization of different feedstocks will be covered, namely, cellulose, carbohydrates, sorbitol, glycerol, ethylene glycol, 1,4-butanediol, isopropanol, ethanol, methanol and formic acid. Although some of these components are nowadays produced from fossil fuels, there are some emerging routes to obtain them from biomasses. Cellulose is a component of lignocellulosic biomasses, and its extraction process can be conducted by ball–milling, acid or alkaline pulping, use of solvents or steam explosion.[9] Carbohydrates, such as glucose, can be obtained by cellulose hydrolysis,[10] while sorbitol derives from glucose hydrogenation and has been also reported to be directly produced from cellulose.[11,12] Glycerol, on the other hand, is a by-product of biodiesel production.[13] Glycerol, as well as ethylene glycol can be obtained by biomass hydrogenolysis.[14] The renewable production of 1,4-butanediol and isopropanol can occur by fermentation of biomasses.[15] Ethanol production as well, mostly comes from biomass fermentation.[16] The gasification of biomass followed by the upgrade of the

[a] Dr. A. Fasolini,+ Dr. G. Martelli,+ Dr. A. Piazzi, Dr. M. Curcio, Dr. J. De Maron, Prof. F. Basile, Prof. R. Mazzoni
Department of Industrial Chemistry "Toso Montanari", University of Bologna
via Gobetti, 85 40129 Bologna, Italy
E-mail: rita.mazzoni@unibo.it

[b] Dr. A. Fasolini,+ Dr. G. Martelli,+ Dr. A. Piazzi, Dr. M. Curcio, Dr. J. De Maron, Prof. F. Basile, Prof. R. Mazzoni
Center for Chemical Catalysis – C3
University of Bologna
viale Risorgimento 4 40136 Bologna, Italy

[c] Dr. A. Fasolini,+ Dr. J. De Maron, Prof. F. Basile, Prof. R. Mazzoni
Interdepartmental Centre for Industrial Research, Renewable Sources Environment, Sea, Energy (CIRI-FRAME)
University of Bologna
viale Risorgimento, 4 40136 Bologna, Italy

[+] Andrea Fasolini and Giulia Martelli contributed equally to this paper.

© 2024 The Author(s). ChemCatChem published by Wiley-VCH GmbH. This is an open access article under the terms of the Creative Commons Attribution Non-Commercial License, which permits use, distribution and reproduction in any medium, provided the original work is properly cited and is not used for commercial purposes.

© 2024 The Author(s). ChemCatChem published by Wiley-VCH GmbH

18673899, 2024, 17, Downloaded from https://chemistry-europe.onlinelibrary.wiley.com/doi/10.1002/cctc.202400393 by CochraneItalia, Wiley Online Library on [25/03/2025]. See the Terms and Conditions (https://onlinelibrary.wiley.com/terms-and-conditions) on Wiley Online Library for rules of use; OA articles are governed by the applicable Creative Commons License

produced gas yields methanol. Finally formic acid can be obtained from biomasses via hydrolysis wet oxidation or ethanol oxidation.[17,18] Moreover, formic acid is a co–product of levulinic acid production from biomasses and sugars.[19,20]

In this context, the so–called aqueous phase reforming (APR) is a catalytic process that employs a catalyst to convert biomasses or biomass–derived feedstocks to hydrogen at relatively low temperatures (200–250 °C) and in aqueous phase (1).[21–26]

$$C_xH_{2y}O_z + yH_2O \rightarrow (x+y)H_2 + xCO_2 \quad (1)$$

Which derives from the consecutive reactions of substrate reforming and water gas shift reaction:

$$C_xH_{2y}O_z \rightarrow yH_2 + xCO \quad (2)$$

$$CO + H_2O \rightarrow H_2 + CO_2 \quad (3)$$

Aqueous phase reforming was first studied by Dumesic *et al.* more than 20 years ago[27] and since then has shown a blossoming of developments in the fields of catalysts and feedstocks.[28–32]

The employment of APR comes with several advantages, as the steam reforming of hydrocarbons typically takes place in the vapor phase. However, the endothermic reforming of oxygenated hydrocarbons is favoured also at lower temperatures allowing to carry out the process in liquid phase.[22]

Compared to classical methods for hydrogen production from fossil fuels (such as natural gas reforming) or biomasses (i.e. gasification), the employment of lower temperatures allows to use water–based feedstocks avoiding energy intensive water vaporization, reduces energy consumption, and favours the occurrence of the water gas shift reaction, which drastically reduces the CO content while increasing the hydrogen one. In addition, low temperature disfavours decomposition reactions of alcohols or carbohydrates. Moreover, the oxygenated biomasses or biomass derived feedstocks are safer than fossil fuels being non–flammable and non–toxic. The autogenous pressure developed in APR (10–40 bars) is, in addition, compatible with hydrogen purification units such as pressure swing absorption.

Although the use of oxygenated feedstocks allows to reduce the operative temperature, it poses the issue of reaction selectivity. In particular, in these conditions alkane production is favoured over hydrogen and carbon monoxide,[22] and the presence of different bonds (C–H, C–O and C–C) requires the use of tailored catalytic active phase able to push the reaction toward the formation of hydrogen. In particular, C–H and C–C bond cleavage must be preferred over the one of the C–O bond to favour the production of CO and hydrogen. To further increase hydrogen production and reduce the CO content the active phase must also be active in the water gas shift reaction (WGSR), but not in methanation. For this reason different heterogeneous catalysts have been studied, starting from the first one employed by Dumesic *et al.*, i.e., Pt/Al_2O_3.[27] Other than Pt, also Ir, Rh, Ru, Fe, Co, Ni, Pd and Cu have been studied.[22,33] Among them, Ni, Ru, Rh, Fe and Co showed the highest activity toward C–C cleavage but a concurrent high activity toward methanation (Figure 1). The lowest methanation activity was displayed by Pt, Cu and Ir. On the other hand, the WGSR was

Rita Mazzoni received her Ph.D in Chemistry in 2005 from the University of Bologna working on the design of rhodium homogeneous catalysts applied in hydroformilation and hydrosililation. Currently she holds a position as Associate Professor in Inorganic Chemistry at the Department of Industrial Chemistry (University of Bologna). Her main research interests are focused on the rational design of homogeneous catalytic systems for sustainable biomass conversion (e.g. bio–oil mixtures, HFM and bio–ethanol valorization) and energy transition (water oxidation, hydrogen production, acqueous phase reforming) based on noble and Earth–abundant transition metal complexes which combine cyclopentadienone and N-heterocyclic carbene ligands.

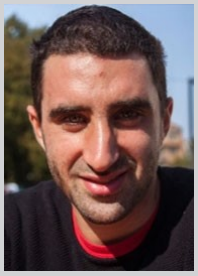

Andrea Fasolini obtained is Master's degree in Industrial Chemistry from the University of Bologna in 2016. He then started his Ph.D. in the laboratory of catalytic processes development with a project on the production of pure hydrogen from methane using membrane reactors. He also took part in projects to produce green hydrogen in liquid and gas phase. He obtained his Ph.D. degree in 2020 and continued his career as a Postdoc fellow starting new projects regarding CO_2 utilization, electrocatalysis, photocatalysis and photoelectrocatalysis. In 2022 he became Research Fellow of the catalytic process development group of the University of Bologna.

Giulia Martelli obtained her PhD in chemical Sciences in 2019 at the University of Bologna with a focus on organic synthesis and biological applications on novel small molecules. Later on, she worked for three years, as a PostDoc fellow, on green chemistry applied to cross–coupling reactions and solid phase peptide synthesis. Since 2021 she covers the role of Scientific Research Technician at Department of Industrial Chemistry, University of Bologna. Her main research interests are the development of methods for characterization of inorganic molecules and materials (solid–state NMR), homogenous catalysis, organometallic chemistry and aqueous–phase reforming of glucose.

© 2024 The Author(s). ChemCatChem published by Wiley-VCH GmbH

18673899, 2024, 17, Downloaded from https://chemistry-europe.onlinelibrary.wiley.com/doi/10.1002/cctc.202400393 by CochraneItalia, Wiley Online Library on [25/03/2025]. See the Terms and Conditions (https://onlinelibrary.wiley.com/terms-and-conditions) on Wiley Online Library for rules of use; OA articles are governed by the applicable Creative Commons License

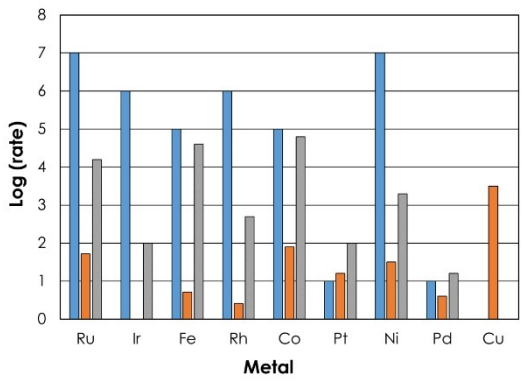

Figure 1. Relative rates of C–C bond breaking (blue), WGSR (red), and methanation (grey) over different metals. Adapted from.[35]

mostly favoured over Cu, Pt, Ru, Ni and Co. Experimental studies carried out on ethylene glycol aqueous phase reforming using group VIII metals supported on SiO_2 showed that the reaction rate followed the order Pt=Ni > Ru > Rh=Pd > Ir.[22,34] However, the highest selectivity toward hydrogen was reported for Pt and Pd.

Concerning biomass derived feedstock, experimental results were obtained using Pt/Al_2O_3 to carry out the APR of methanol, ethylene glycol, glycerol, sorbitol and glucose.[36] Noteworthy, a wide pool of feedstocks have been used to produce hydrogen form aqueous solutions like methanol, formic acid, ethylene glycol, ethanol, glycerol, xylitol, sorbitol, fructose, glucose, sucrose and cellulose. An increase in feedstock complexity resulted in a decrease in hydrogen selectivity, and a concurrent increase in selectivity toward alkanes. The decrease in hydrogen selectivity for more complex molecules is related to the occurrence of stoichiometric reactions occurring at the relatively high temperatures used in APR and that lead to the production of solid products called humins,[37–39] occurring especially at high feed concentrations.

The need for improved selectivity, mechanistic understanding and milder reaction conditions promoted the parallel development of homogeneous catalytic systems for hydrogen production. In general, molecular catalysis prevents alkane and CO formation, providing better selectivity at lower temperatures. However, for these liquid substrates, stability, recover and recyclability of molecular catalysts still remain an important drawback which seems to be partially overcome by catalysts immobilization. On the other hand, the use of homogeneous catalysis is relatively young and still underdeveloped for more complex substrates such as xylitol, sorbitol, fructose, glucose, sucrose and cellulose as biomass derived substrates. In general, the higher the complexity of the substrates, the more the process could benefit from selectivity control and finely tuned design by mechanism understanding. Homogeneous catalysis may thus be the way to reach applicable APR processes providing less harsh reaction conditions. Moreover, although hydrogen production by APR, i.e. dehydrogenation of biomass derived feedstocks, has been mainly carried out using heterogeneous catalysts in light of their easy separation, homogeneous catalysis can help to cope with some issues of this process, such as the difficult interaction between a solid catalyst and a solid reagent (cellulose for instance). Moreover, lower operative temperatures would reduce stoichiometric side reactions such as formation of solid humin products.

Following these considerations, the present review will cover the advancement reported in the homogeneously catalysed dehydrogenation reactions of biomass derived molecules to produce green hydrogen, critically analysing the advantages, flaws and consequent opportunities.

2. Biomass Derived Feedstocks for H_2 Production in Homogeneous Catalysis

2.1. Hydrogen Production from Formic Acid

Being the simplest carboxylic acid, formic acid (FA) holds promise as a Liquid Organic Hydrogen Carrier (LOHC), as its molecular weight allows for a 4.38 wt% gravimetric H_2 capacity. Although such value is modest compared to that of alternative LOHCs like ammonia (17.8 wt%) or methanol (12.1 wt%), its high density and high boiling point appoint FA as an easy–to–handle LOHC with a volumetric H_2 capacity of 53 g L^{-1}, comparable to commercially available compressed H_2 tanks.[40] FA is accessible on large scale, has low toxicity and flammability and can be dehydrogenated in solution at moderate temperatures thanks to a low reaction enthalpy.[41] An efficient FA dehydrogenation reaction would ideally lead to the exclusive production of the desired product H_2 and CO_2, with the latter separated[42] and re-hydrogenated–potentially with H_2 from renewable sources to provide back FA and achieve sustainable and carbon–neutral energy storage and release.[43–44]

However, FA dehydrogenation (FADH) has to compete with a secondary dehydration reaction, that degrades FA into water and CO. From an applicative point of view, carbon monoxide is a highly undesired byproduct as it poisons the electrodes of the fuel cells that convert H_2 into energy, impacting their performance.[45] In the search for the best catalytic systems for FADH, it is thus imperative to maintain an excellent selectivity with respect to the competing dehydration process. In this regard, the use of single–site homogeneous catalysts is highly preferred, since these systems display excellent selectivity towards the dehydrogenation pathway and are less susceptible of poisoning by traces of carbon monoxide than their heterogeneous counterparts.

The field of homogeneous catalysis for FADH has witnessed a massive development in the last years, with a multitude of breakthrough advancements and a considerable number of excellent reviews focusing both on the catalysts structure–activity relationship[46–53] and on the technical evaluation of the most suitable candidates to be implemented in real–life devices.[54–57] The following paragraph will provide an overview of the most recent and best performing homogeneous catalytic systems for FADH, differentiated based on the nature of metal center, with a final outlook on the possible directions that

© 2024 The Author(s). ChemCatChem published by Wiley-VCH GmbH

18673899, 2024, 17, Downloaded from https://chemistry-europe.onlinelibrary.wiley.com/doi/10.1002/cctc.202400393 by CochraneItalia, Wiley Online Library on [25/03/2025]. See the Terms and Conditions (https://onlinelibrary.wiley.com/terms-and-conditions) on Wiley Online Library for rules of use; OA articles are governed by the applicable Creative Commons License

might be undertaken in future years. Structures of noble metal based catalysts in this paragraph are reported in Figure 2.

Since pioneering studies from Coffey,[58] iridium complexes have held the title of best performing FADH catalysts in the last two decades,[59–63] and this trend was maintained even in more recent examples, in which the metal center is often chelated by polydentate ligands incorporating combinations of *N*-, *O*-, or *P*-donors.

Kawanami and co-workers reported a series of [Ir-(Cp*)(bipy)]$^{2+}$ complexes provided with differently substituted bipyridine ligands competent in highly selective FADH.[64] Catalysts **Ir 1** and **Ir 2**, in which the bipy ligand bears amino or alkyl–amino groups in the *para* positions showed the highest reactivities in 1.0 M $FA_{(aq)}$, reaching TOF values of 10100 h^{-1} and 12700 h^{-1} at 60 °C, respectively. Combined with a temperature increase at 80 °C, addition of NaOH allowed catalyst **Ir 2** to reach a TOF of 115500 h^{-1} in 3.0 M $FA_{(aq)}$. Importantly, despite **Ir 2** showing higher TOF values with respect to **Ir 1**, the latter displayed superior stability and achieved TON values higher of one order of magnitude, up to an optimized 402000 in 5.0 M $FA_{(aq)}$.

Bioinspired Ir complexes incorporating pyrazole ligands bearing pendant N-heterocycles were investigated by Bao, Li and co-workers.[65] Complex **Ir 3** achieved a TOF of 46510 h^{-1} at 90 °C in 1.0 M $FA_{(aq)}$ and proved to be stable also in concentrated systems (6.0 M FA) reaching a maximum TOF of 8250 h^{-1} at 60 °C. Mechanistic studies highlighted the key role played by the appended N-heterocycles in the outer coordination sphere in stabilizing the transition states and their cooperativity as proton relays for enhanced proton transfer processes.

Transition–state stabilization through remote ligand N-groups was exploited by Li and co-workers in the Ir(Cp*)(thqd) complex **Ir 4** (thqd = tetrahydroquinoxaline–dioximine).[66] Thanks to a careful ligand design, the presence of β-NH units allows the establishment of a low–energy H–bonded dehydration transition state. This in turn endowes such complex with high activity in FADH, reaching a TON of 100000 and a TOF of 80000 h^{-1} at 60 °C in 1.0 M $FA_{(aq)}$. The catalyst proved to be highly robust and maintained an unaltered reactivity both over ten consecutive cycles, achieving a cumulative TON of 1000000, while a higher initial TOF of 337500 h^{-1} was observed at 80 °C in 4.0 M $FA_{(aq)}$.

Fischmeister and co-workers reported the Ir–(dpa) complex **Ir 5** (dpa = dipyridylamine) as an additive–free FADH catalyst.[67] Mechanistic investigations unveiled the key cooperation between the bridging NH and the sulfate counterion both in substrate activation and transition state stabilization. The catalytic system successfully converted 3.0 M $FA_{(aq)}$ reaching a TON of 84453 and a TOF of 39274 h^{-1} at 90 °C and its stability was tested over consecutive catalytic runs with a slow loss in activity observed after the second cycle. Notably, the strong electron–donating properties of the doubly dimethylamino–

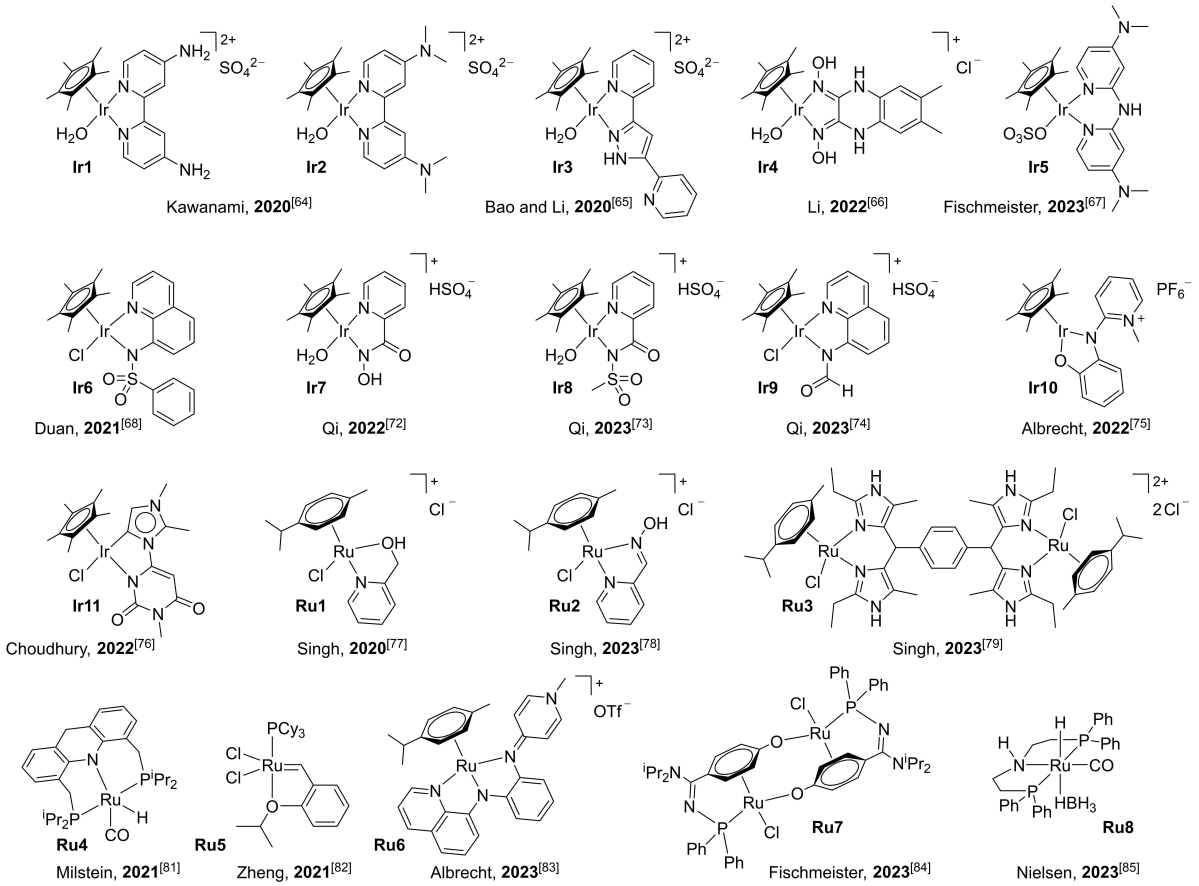

Figure 2. Noble metal based homogeneous catalysts employed for hydrogen production from FA.

© 2024 The Author(s). ChemCatChem published by Wiley-VCH GmbH

18673899, 2024, 17, Downloaded from https://chemistry-europe.onlinelibrary.wiley.com/doi/10.1002/cctc.202400393 by CochraneItalia, Wiley Online Library on [25/03/2025]. See the Terms and Conditions (https://onlinelibrary.wiley.com/terms-and-conditions) on Wiley Online Library for rules of use; OA articles are governed by the applicable Creative Commons License

substituted dipyridylamine ligand allowed complex **Ir5** to dehydrogenate neat FA in the absence of any additives and displaying one of the highest activities reported to date, with a TOF of 11373 h^{-1}.

Duan and co-workers studied Ir(Cp*) complexes bearing rigid aminoquinolinesulfonamide chelates.[68] Such catalysts effectively dehydrogenated FA, demonstrating in the case of complex **Ir6** a TON of 600000 in 6.0 M FA at 60 °C. Experimental kinetic studies combined to computational simulations revealed the pivotal role of electron–poor and electron–rich substituents in enhancing the β-hydride elimination step or the protonation of the Ir–H, respectively.

Inspired by previous work on Ir–picolinamide complexes,[69–71] Qi and co-workers investigated the reactivity of iridium complexes supported by picolinamide ligands bearing a combination of *N*-methyl, *N*-hydroxy or *N*-methoxy substituents toward FADH.[72] Among them, complex **Ir7** supported by an *N*-hydroxy–picolinamide provided the best performance with a TOF of 90625 h^{-1} at 80 °C and a cumulative TON of 120520 over seven catalytic runs. In a follow up study, the picolinamide framework was edited through the addition of a sulfonamide ligand featuring strong sigma–donation on the coordinated amide nitrogen.[73] This led to the development of the highly active methyl–sulfonyl–picolinamide iridium complex **Ir8**, reaching a TON of 151000 and a TOF of 195000 h^{-1} at 90 °C. The system was tested over multiple catalytic runs, showing a resilient reactivity despite a gradual loss in activity after the first eight runs. To combine the influence of the enhanced sigma donation and the reactivity reported for quinoline-based systems,[68] the authors developed complex **Ir9** in which the iridium center is coordinated by an *N*-8-quinolinylformamide ligand.[74] Complex **Ir9** successfully catalyzed FADH, providing upon careful optimization of the reaction conditions a TOF of 206250 h^{-1} in a 1:1 FA:HCOONa mixture at 90 °C. Quinolylformamide emerged as a non-innocent proton–responsive ligand which could be deprotonated at the formyl position (pK_a = 3.60). Computational mechanistic studies supported a transition state–stabilizing interaction between the thus formed carbanion and water solvent molecules.

Albrecht and co-workers operated a careful tuning of the coordinating properties of an *N*,*O* chelate, developing the Ir(Cp*) complex **Ir10** in which the metal center is coordinated by a phenoxy–substituted pyridylidene–amine (PPYE) ligand, characterized by two limiting resonance structures: π-acidic zwitterionic or π-basic quinoidal.[75] With an unusual two–legged piano stool structure, **Ir10** is a stable 16 e^- complex, as confirmed by the lack of solvent coordination when precipitated from dimethylsulfoxide (DMSO). The vacant coordination site and flexible donor properties of the PPYE ligand confer **Ir10** an impressive efficiency in FADH, reaching under continuous FA addition a TON of 3000000 in 35 h and a steady TOF value of 77000 h^{-1} in 1.0 M FA, 1.0 M HCOOLi in DMSO at 80 °C.

Choudhury and co-workers reported the water soluble complex **Ir11**, in which the Ir center is coordinated by an uracil–functionalized abnormal NHC ligand.[76] Such compound displayed catalytic activity in both CO_2 hydrogenation and FADH, reaching for the latter a TON of 6134 and a TOF of 73619 h^{-1} in 0.7 M FA, 0.3 M HCOOK at 80 °C.

Despite the striking success of iridium catalysts, ruthenium complexes maintain their status as compounds of interest based on the higher availability (~100×) and lower cost (~0.1×) of the required Ru precursors. Furthermore, recent Ru–based catalytic systems displayed unprecedented performances that match or even outperform some of their Ir counterparts.

Singh and co-workers investigated a series of mononuclear Ru(*p*-cymene) complexes supported by pyridine-derived ligands bearing oxygen- or nitrogen-chelating donors.[77,78] Out of the numerous candidates studied, complexes **Ru1** and **Ru2** proved active and highly stable, displaying cumulative TON values of 6050 over 7 runs and 13000 over 26 runs at 90 °C, respectively. In related studies, the authors developed mono- and dinuclear Ru(*p*-cymene)-bis (imidazolyl) methane complexes and evaluated their promise as FADH catalysts.[79,80] Dinuclear complexes resulted more active than their mononuclear counterparts, with complex **Ru3** providing the best catalytic performance and achieving a TON of 93200 and a TOF of 1993 h^{-1}/Ru center at 90 °C in 2.0 M FA, 0.8 M HCOONa.

The Ru(9H-acridine) pincer complex **Ru4** reported by Milstein and coworkers represents a rare example of catalysts competent in the base- and additive-free dehydrogenation of neat FA.[81] Despite displaying catalytic activity already at room temperature, such complex provided the best performance at higher temperatures up to 95 °C with a TOF of 3067 h^{-1} and a TON of 1701150. The high catalyst stability was tested both in a large–scale experiment with 1.5 kg FA decomposed into 1560 L of H_2/CO_2 mixture over 19 days and in a closed–vessel reaction that yielded up to 100 bar of gas product mixture.

Commercially–available olefin metathesis catalysts were tested in FADH by Zheng and co-workers.[82] First-generation Hoveyda–Grubbs catalyst **Ru5** outperformed the other complexes, providing a TON of 36356. Mechanistic studies by NMR spectroscopy supported the formation of an initial $Ru(H)_2$ complex evolving sequentially into a $Ru(H)(H_2O)$ intermediate and a Ru(H)(HCOO) species, that restored the initial Ru–dihydride through β-hydride elimination.

Appropriately engineering a pyridylidene–amine motif,[75,83] Albrecht and co-workers developed complex **Ru6** in which the Ru center is supported by an NNN chelate adopting a quinoidal structure. Complex **Ru6** demonstrated high activity in FADH, reaching a TOF of 9200 h^{-1} in DMSO at 80 °C, despite suffering from a modest stability with a TON of 2200.

The dimeric Ru complex **Ru7** developed by Fischmeister and co-workers selectively provided H_2 by decomposition of a 2.4 M FA solution in DMSO at 90 °C in the absence of additives or bases, reaching a TOF of 202 h^{-1} and a TON of 173.[84] Importantly, complex **Ru7** resulted effective also in the reverse reaction – *i.e.* CO_2 hydrogenation – and retained its activity after three hydrogen storage and release cycles, demonstrating potential toward H_2 transport and delivery.

Nielsen and co-workers investigated an efficient FADH catalytic system combining the Ru–PNP complex **Ru8** to the ionic liquid 1-butyl-3-methylimidazolium acetate ([BMIM][OAc]).[85] Selective H_2 production was observed at 95 °C

© 2024 The Author(s). ChemCatChem published by Wiley-VCH GmbH

18673899, 2024, 17, Downloaded from https://chemistry-europe.onlinelibrary.wiley.com/doi/10.1002/cctc.202400393 by CochraneItalia, Wiley Online Library on [25/03/2025]. See the Terms and Conditions (https://onlinelibrary.wiley.com/terms-and-conditions) on Wiley Online Library for rules of use; OA articles are governed by the applicable Creative Commons License

upon continuous FA supply (10 mL h^{-1}) corresponding to a TOF of 10600 h^{-1}. The remarkable stability and unvaried catalytic activity of the **Ru 8**/[BMIM][OAc] mixture upon several weeks of storage prompted a large–scale experiment in which 14.5 L of FA were successfully hydrogenated over 112 days, providing the record TON value of 18100000.

Parallel to the development of efficient noble metal catalysts, considerable efforts were directed to the development of Earth–abundant metal systems (Figure 3) such as iron,[86–95] manganese,[96,97] cobalt,[98,99] nickel,[100,101] and copper[102–106] as attractive inexpensive alternatives. In recent years, the following main advancements were reported regarding non–noble metal FADH catalysts.

Hazari and co-workers developed a family of iron complexes supported by PNP pincer ligands.[107–109] Complex **Fe 1**, in which the bridging N-donor bears a methyl substituent, demonstrated impressive reactivity and stability reaching a TON of 100000 and a TOF of 62000 h^{-1} in the dehydrogenation of additive–free FA at 90 °C in toluene : tBuOH.[107] Interestingly, this catalyst is a rare example in which metal–ligand cooperation is not a strict requirement to achieve high reactivity. In a subsequent report, the authors carried out a detailed investigation of the reactivity of the Fe–H complex **Fe 2**, a (pre) catalyst for hydrogenation and dehydrogenation reactions.[108] The study led to the identification of key coordinatively unsaturated intermediates linked to catalyst deactivation that stabilize through the formation of dimeric species. This mechanistic understanding was pivotal to determine that the addition of small ligands like PMe_3 can disfavor the dimerization pathway, thus increasing the catalyst lifetime in FADH.

Compared to the 15-year literature on iron–based compounds, reports testing the potential of manganese complexes toward FADH remained surprisingly limited, with early work from Boncella and co-workers being the only examples up to 2019.[96,97] Inspired by this, in recent years Beller and co-workers conducted an extensive research activity dedicated to Mn catalysts for FADH.[110–113] An initial report involved the development of Mn(I)(imidazoline–pyridine) complex **Mn 1**, which proved catalytically active and reached a maximum TON of 5763 in 1.5 M phosphate buffer at 90 °C after 45 h of continuous FA supply, despite suffering a moderate selectivity.[110] Preliminary experimental mechanistic studies proposed the β-hydride elimination of the Mn–formate intermediate being rate limiting, hypothesis recently corroborated by a detailed computational investigation that led to an estimated 19.0 kcal mol^{-1} activation energy barrier for such process.[114] Improved reactivity and selectivity with respect to CO production were later observed adopting the related Mn(bis–imidazoline) complex **Mn 2**.[111] The authors reported a major advancement in FADH when testing the Mn–pincer complex **Mn 3**.[112] Despite being Mn–based, such compound displayed high reactivity and stability with a single–run TON of 29400 and a cumulative TON of 676700 over ten consecutive runs at 90 °C in a H_2O : THF mixture using lysine as an additive. Most importantly, complex **Mn 3** was found to be catalytically active not only in FADH, but also in the reverse CO_2 hydrogenation reaction with a remarkable cumulative TON of 2050000. This prompted catalyst testing in the combined hydrogen storage–release process with 82 % H_2 evolution efficiency and > 99.9 % CO_2 retention over ten cycles.

These results were further expanded in a subsequent study in which complex **Mn 4** was used to catalyze HCOOK DH as a semireaction in the reversible H_2 storage–release process exploiting the interconversion between potassium carbonate and potassium formate.[113]

Huang and co-workers reported the pyridine–based Mn-pincer complex **Mn 5** as highly active in FADH, displaying a TON of 15200 and a TOF of 2086 h^{-1} exploiting a FA–Et_3N mixture at 90 °C in DMSO.[115] The system high selectivity was attributed to an effective metal–ligand cooperativity, maintaining the metal oxidation state unaltered, that was supported by the isolation of Mn–formate and Mn–hydrido intermediates.

The first Co-based complex able to catalyze additive–free FADH was reported by Cantat and co-workers.[116] Compound **Co 1** showed a remarkable activity among Co–catalysts, reaching a cumulative TON of 458 over three consecutive runs and an initial TOF of 4020 h^{-1} in 0.06 M FA in 1,4-dioxane at 80 °C.

More recently, Tsai and co-workers reported the Co–triphos complex **Co 2** as a FADH catalyst, achieving a TON of 1735 and a TOF of 483 h^{-1} in 2.0 M FA in acetonitrile at 70 °C.[117] A careful combination of experimental and theoretical mechanistic studies led to the proposition of two competing reaction pathways starting from the same Co(II)H intermediate and involving either i) substrate deprotonation or ii) dimerization and subsequent reductive elimination to Co(I).

As a general consideration formic acid is currently one the most promising LOHCs since it combines a high H_2 gravimetric capacity with low hazardousness and toxicity and high boiling point, which make it ideal for large–scale applications. The crucial advantage that FA holds against competing LOHCs lies in the recyclability of its dehydrogenation product CO_2, which can effectively lead to a net zero–carbon cycle and thus achieve a long–sought goal in sustainable energy production and CO_2

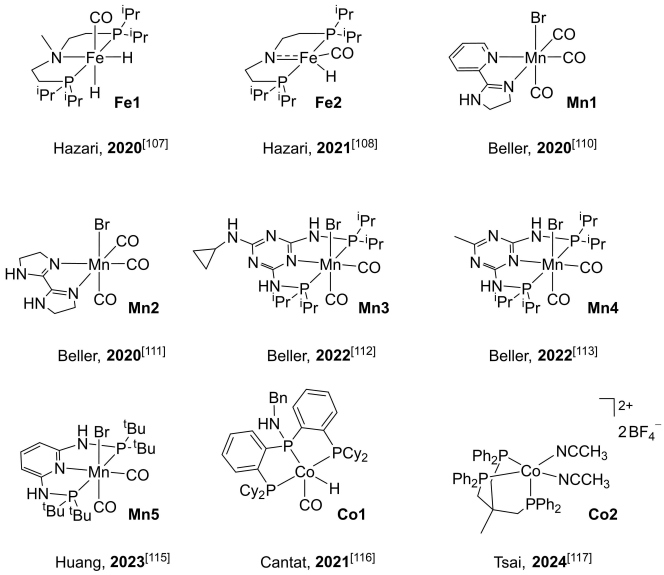

Figure 3. Earth abundant metal based homogeneous catalysts employed for hydrogen production from FA.

© 2024 The Author(s). ChemCatChem published by Wiley-VCH GmbH

18673899, 2024, 17, Downloaded from https://chemistry-europe.onlinelibrary.wiley.com/doi/10.1002/cctc.202400393 by CochraneItalia, Wiley Online Library on [25/03/2025]. See the Terms and Conditions (https://onlinelibrary.wiley.com/terms-and-conditions) on Wiley Online Library for rules of use; OA articles are governed by the applicable Creative Commons License

utilization. The last years witnessed impressive advancements in the field of homogeneously catalysed FADH, with improved catalytic systems based on both noble- and base-metals displaying astounding performances often driven by finely tuned ligands or unconventional mechanistic routes. However, critical aspects have yet to be addressed to support the effective implementation of such systems in practical applications.

i) Catalyst activity and stability should necessarily be taken into consideration during the evaluation of FADH catalytic systems for prospective applications, as they are related to the amount of H_2 supplied over time and the lifespan of the targeted device, but are far from being sufficient on their own. To include economic factors such as the cost of the raw materials and ligand preparation in the evaluation, catalyst price normalized parameters were recently introduced that highlighted how moderately performing simple non–precious metal catalysts could be overall equally – or more – appealing than high performing catalysts based on noble metals and complex ligands.[46,55]
ii) Homogeneous FADH catalytic systems maintain excellent CO_2:CO selectivity, highly disfavoring the competitive dehydration pathways. However, their operative conditions are still far from being optimal since the majority of the catalysts reported in the last years require a basic reaction environment, oftentimes accompanied by additives, to achieve good performances. In contrast, only a limited number of selected Ru– and Ir– based examples displayed sufficient tolerance and reactivity in neat FA to conduct the dehydrogenation reaction.

It can be thus foreseen that future research on homogeneous FADH will target catalysts that are not limited to showing sufficient activity and stability to ensure a prolonged device operation, but do also include readily accessible ligand frameworks and inexpensive Earth–abundant metals. Advanced FADH catalytic systems must also provide efficient reactivity in neat FA and in the absence of any additives in order to maximize the system hydrogen capacity.

2.2. Hydrogen Production from Alcohols: MeOH, EtOH, Isopropanol

First highlighted by Schneider in 2009,[118] homogeneously catalysed acceptorless dehydrogenation of alcohol represented, since then, a succulent perspective within the framework of H_2 synthesis and storage. The subject crossed the decades maintaining a high scientific relevance as proven by the number of reviews published up to 2022.[119,51] Together with formic acid, methanol is the most reviewed substrate due to its high suitability in the so called *methanol economy* (methanol dehydrogenation and methanol production) especially while concerning the complete dehydrogenation of methanol to inert CO_2 and vice versa.[120] In the most recent review (2022), Kumar, Daw and Milstein[51] very well summarized homogeneous catalysts reported for (de)hydrogenative transformations (Figure 4) with the general statement that homogeneous catalysis allows the processes to occur under milder conditions favouring, at the same time, the understanding of the reaction mechanisms with the aim to develop new and more efficient catalysts. Methanol is a stable liquid with low viscosity and, in theory, a high gravimetric hydrogen capacity (up to 12 wt% considering the aqueous methanol reforming). As depicted in Figure 4, the homogeneous aqueous methanol reforming reaction requires three main steps: i) dehydrogenation of methanol to formaldehyde; ii) its reaction with water to generate formic acid, and iii) dehydrogenation of formic acid to H_2 and CO_2.

Other reviews dealing with the same subject covered the period up to 2018.[121–123] Although aqueous methanol reforming represents to date the most investigated application of alcohols as hydrogen storage, the more general concept of applicability of methanol and other alcohols in acceptorless dehydrogenation mediated by transition metal complexes and the related transformations in chemical synthesis where the aim is hydrogen production or co–production, has been also widely described.[124,125]

In this paragraph a short summary on results reported until 2022 will be followed by a deeper description of recent developments.

Pincer bifunctional ruthenium–based catalysts **Ru 8–10** for aqueous methanol reforming were developed by Beller and coworkers.[126] They produced, in the presence of a base, up to 3 equiv of hydrogen gas ($CH_3OH + H_2O = 3H_2 + CO_2$) at temperatures ranging 65–95 °C, significantly milder than those adopted in heterogeneous processes (>200 °C). Several mechanistic insights were found for the role of the base, solvent, and metal–ligand cooperation.[127–131] Equivalent interest was devoted to an anionic ruthenium complex **Ru 11** employed by Grutzmacher group.[132–135] Despite a lower TOF, such catalyst leads to a higher conversion and it does not need any base or additive. Later on, Beller applied a dual catalytic system based on the ruthenium–MACHO pincer complex and the ruthenium bisphosphine dihydride **Ru 12–13** showing a positive synergistic effect and higher catalytic activity.[136] Another class of non-innocent PNN pincer ligands (**Ru 14**) was soon after introduced in base activated ruthenium complexes active in the dehydrogenation of methanol/water by Milstein[137] and later, in 2016, it was the time of Reek's group which explored the activity of ruthenium carbonyl complexes **Ru 15**.[138]

Computational studies revealed, in general, two mechanistic pathways for the aqueous reforming dehydrogenation of methanol mediated by molecular ruthenium complexes: metal–centered and metal–ligand cooperative. As recently reviewed by Sinha and de Bruin[139] discerning between these two possible pathways by DFT calculation is not trivial since results strongly depend on input employed (e.g. solvent effects,[140] metal–ligand cooperativity, different geometries, and electronic structure of the metal). More in details, solvent effects, control on the basicity of the ligands and acidity of the metal center and hydridicity of the M–H bond formed during the substrate dehydrogenation are important parameters in order to discern if the reaction proceeds through a metal–ligand cooperation or through a metal centered type mechanism.

© 2024 The Author(s). ChemCatChem published by Wiley-VCH GmbH

18673899, 2024, 17, Downloaded from https://chemistry-europe.onlinelibrary.wiley.com/doi/10.1002/cctc.202400393 by CochraneItalia, Wiley Online Library on [25/03/2025]. See the Terms and Conditions (https://onlinelibrary.wiley.com/terms-and-conditions) on Wiley Online Library for rules of use; OA articles are governed by the applicable Creative Commons License

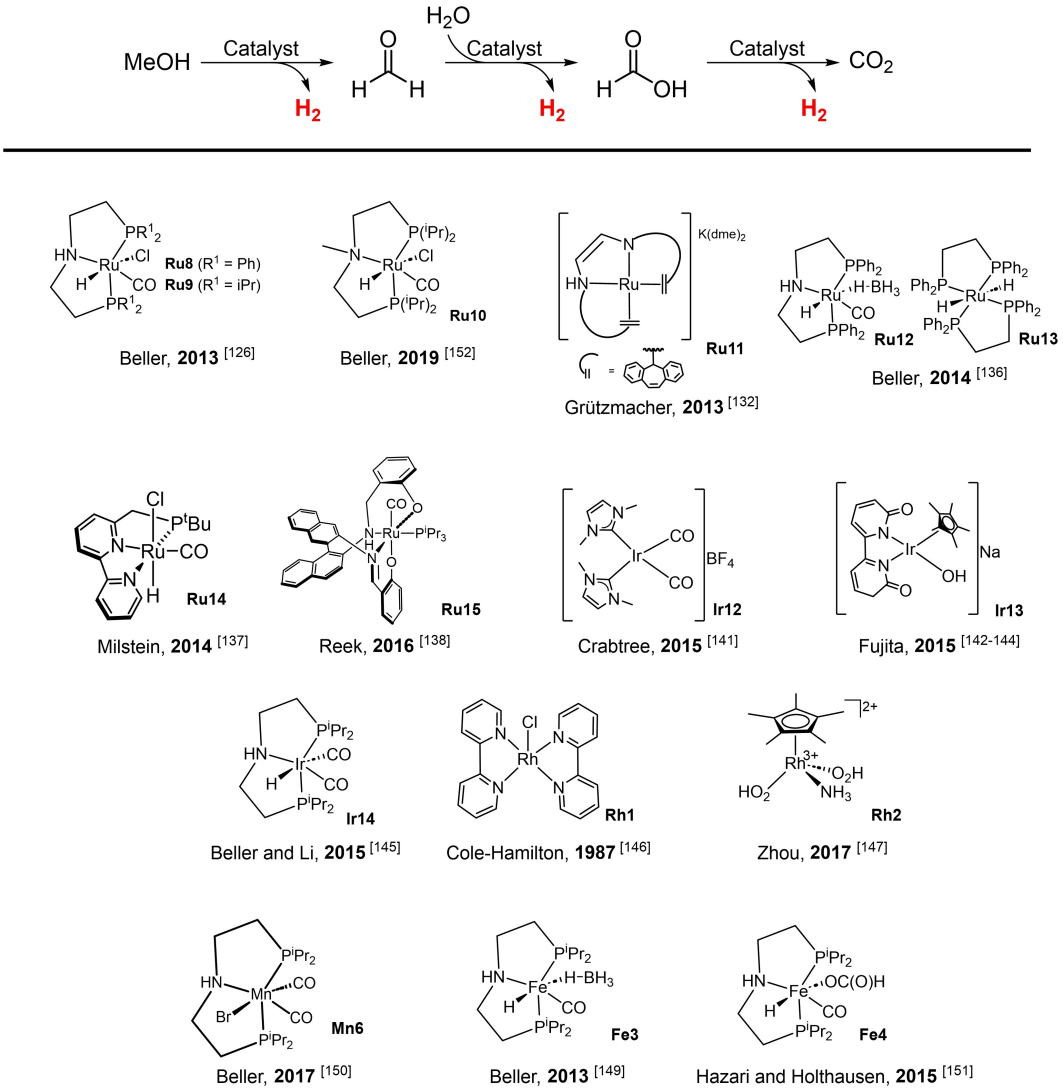

Figure 4. Homogeneous catalysts employed in aqueous methanol reforming before 2022.

Group 9 complexes were also found active, albeit less than ruthenium based ones, in the aqueous methanol reforming by Crabtree (iridium N-heterocyclic carbene complex **Ir 12**),[141] Fujita and Yamaguchi (pH-responsive iridium bipyridonate complex **Ir 13**),[142–144] Beller (iridium PNP–MACHO complex **Ir 14**)[145] all of them working in the presence of a base. Cole–Hamilton ([Rh(2,2-bipyridyl)$_2$]Cl) **Rh 1**,[146] Zhou ([Cp*Rh-(NH$_3$)(H$_2$O)$_2$]$^{2+}$) **Rh 2**.[147]

As the most active group in the field, Beller and co-workers lately progressed toward the development of catalytic systems for aqueous methanol reforming based on earth abundant metals such as iron and manganese (**Fe 3**, **Mn 6**). The subject was extensively reviewed by Dow[148] in 2021. Highlighting the importance of replacement of nobel metal with the less toxic and more available first row transition metal complexes, it describes bifunctional catalysis and pincer complexes bearing non-innocent ligands that furnish a path to exploit a similar catalytic behaviour as for ruthenium complexes although with overall lower stability.[149,150] In the meantime Fe–PNP pincer catalyst **Fe 4** were published by Bernskoetter, Hazari, and Holthausen which, unlike the previous that need basic environment, work under acidic conditions.[151]

Taking advantage of this state of the art, recent advances in aqueous methanol reforming reveal the effect of catalysts combination and the use of additives as new available paths to improve efficiency and avoid a basic reaction environment. Furthermore, variable immobilization techniques allow to move the process in gas phase towards a continuous steam reforming.

Lower reaction temperature and base concentration can be applied to the process while working with the bi-catalytic system in a cascade reaction developed by Beller and co-workers.[152] Combining a catalyst efficient in methanol dehydrogenation (**Ru 9** in Figure 4) with a series of catalysts more active in the dehydrogenation of formic acid (nine among Ru, Ir, and Fe complexes) the best synergistic effect was observed applying ruthenium complexes **Ru 9** and **Ru 10**. A comprehensive description of the rational design of homogeneous catalysts

© 2024 The Author(s). ChemCatChem published by Wiley-VCH GmbH

18673899, 2024, 17, Downloaded from https://chemistry-europe.onlinelibrary.wiley.com/doi/10.1002/cctc.202400393 by CochraneItalia, Wiley Online Library on [25/03/2025]. See the Terms and Conditions (https://onlinelibrary.wiley.com/terms-and-conditions) on Wiley Online Library for rules of use; OA articles are governed by the applicable Creative Commons License

with a focus on catalyst optimization for bi-catalytic cascade or tandem reactions to promote in a single pot and under same reaction conditions, different transformation, candidate this work as an essential reference for the future design of new solutions for this process.

Taking inspiration from bi-catalytic systems combining enzyme and Ir or Ru based catalysts,[153,154] and aware of formic acid dehydrogenation being the rate determining step, the authors realized that if formic acid accumulates in the reaction mixture, the catalyst can be deactivated due to acidic conditions. Indeed, the bi-catalytic system reported in Scheme 1 demonstrated how the first PNP pincer ruthenium catalyst **Ru 9** (which operates efficiently only at high base concentration, 8 M KOH) synergistically work with **Ru 10** (competent in the dehydrogenation of formic acid) with a significant reduction of base required for the process [reaction conditions: MeOH (9.0 mL), H_2O (1.0 mL), Triglyme (4.0 mL), KOH (40 mmol), T = 92.5 °C, reaction time 3 h)].

The combination of **Ru 9** and **Ru 10** in a 1:1 ratio almost doubled the hydrogen production (up to 700 mL). A further decrease of base to 5 mmol (20 mL triglyme) resulted in another advantage shortening the initiation phase and increasing the hydrogen production from 14.3 to 10.5 mL/h. The base/solvent ratio also impacted the reaction phases. The bi-catalytic system produces a mixture of H_2 and CO_2 in 3:1 ratio and, under the best conditions, is 1.5 time more active than the mono–catalytic ones (TOF **Ru 9** = 142 h^{-1}; TOF **Ru 10** = 168 h^{-1}) further showing the importance in methanol APR of speeding up the dehydrogenation of formic acid.

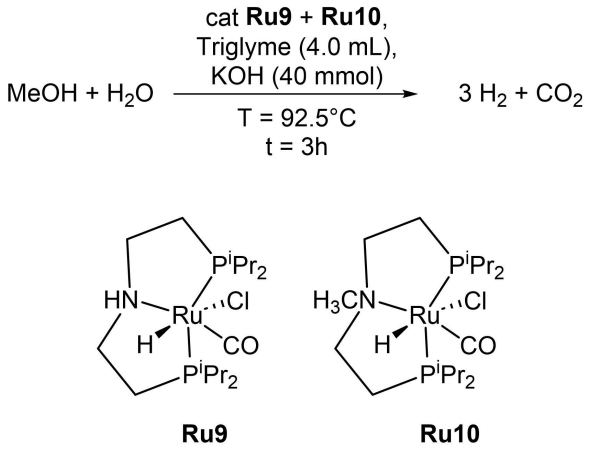

Scheme 1. Bi-catalytic system which reduce the requirement of base in the dehydrogenation of methanol.[152]

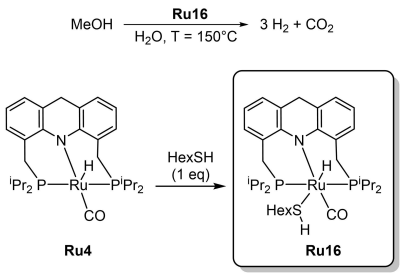

Scheme 2. Thiol promoted ruthenium pincer catalysed aqueous reforming of methanol.[155]

A novel strategy to prevent the use of base in the reaction was lately illustrated by Milstein and co-workers exploiting an acridine–based ruthenium pincer complex (Scheme 2).

As detailed above, to realize a base–free methanol APR reaction the catalyst needs to be able to dehydrogenate methanol without base activation. Furthermore, it is required to be acid resistant in order to be able to continue the dehydrogenation step even in the presence of increasing amount of formic acid and CO_2 gas.

Most exciting results arose from the use of a catalytic amount of thiol as an additive (ratio 1:1 with the catalyst), which increased the reactivity of the system by 2 orders of magnitude (> 80–fold), maintaining activity for over 3 weeks, producing 10 L of gas, thus achieving an impressive TON of over 130000 in H_2 (yield 96% based on the amount of water) and a TOF up to 643 h^{-1}.[155] Notably, the system works at 150 °C in a closed reactor without the need for additional solvents.

Reactivity and control experiments demonstrated that **Ru 16** can be the actual pre–catalyst. An additive free reforming process is also possible with the preformed thiol–derived species. Experimental evidences were also supported by computational studies, unravelling that the mechanism follows an outer sphere dehydrogenation process, with thiolate as assisting ligand.

As depicted in Scheme 3, the mechanism involves the ruthenium hydride complex **Ru 4** in the CO_2/H_2 production from formic acid (third and last step of the whole reaction – the cycle on left side) and the ruthenium thiolate complexes **Ru 16** in the ligand assisted outer sphere dehydrogenation of methanol and methanediol, the latter formed by formaldehyde and water (first and second step of hydrogen production on the right side catalytic cycle). Thiol and thiolate assume a unique and critical role in favouring and improving the efficiency of base–free methanol APR. Nevertheless, in this system the acridine moiety and **Ru 4** complex are also crucial for the operating principles of the mechanism. Indeed, the **Ru 4** ligand framework is resistant to acidic conditions, but also allows the thiolate to access the complex. The promising tunability of acridine ligands, the stability of the relative complexes and the possibility to avoid the use of large amount of base or added solvents, make this process more sustainable and environmentally friendly than the ones previously described, paving the way for further development of the reaction parameters and catalyst's stability to decomposition during the APR reaction, with the final aim of scaling up the process to larger systems.

Another interesting approach to methanol APR has been recently found in the immobilization of molecular complexes to obtain reforming materials to be employed in the vapor phase.[156]

In the first example the homogeneous [RuH(CO)Cl(HN-(C_2H_4Pi–Pr_2)$_2$)] (**Ru 9** in Figure 4) PNP pincer complex was chosen due to its high productivity (> 350,000 turn overs), stability (> 3 weeks) and selectivity. The catalyst works with an inner sphere mechanism and is among those systems that compulsory needs

© 2024 The Author(s). ChemCatChem published by Wiley-VCH GmbH

18673899, 2024, 17, Downloaded from https://chemistry-europe.onlinelibrary.wiley.com/doi/10.1002/cctc.202400393 by CochraneItalia, Wiley Online Library on [25/03/2025]. See the Terms and Conditions (https://onlinelibrary.wiley.com/terms-and-conditions) on Wiley Online Library for rules of use; OA articles are governed by the applicable Creative Commons License

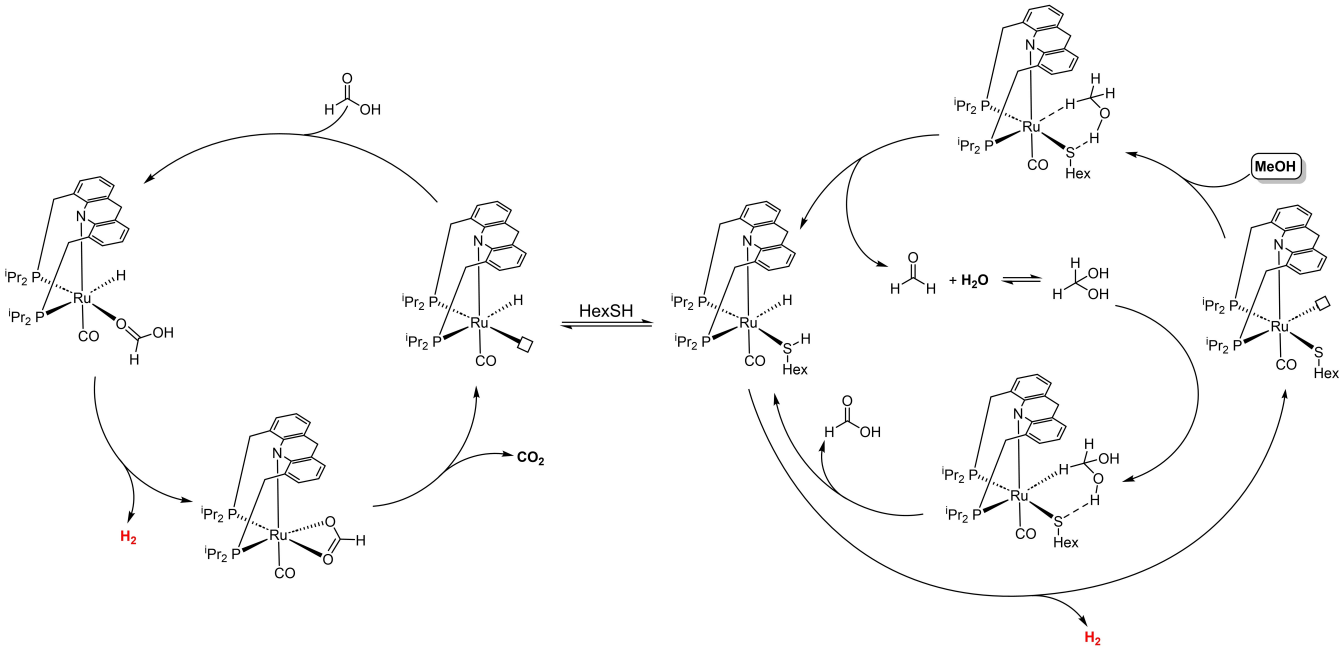

Scheme 3. Proposed mechanism of methanol reforming based on both **Ru 4** and the ruthenium thiol(ate) complexes.[155]

the base to activate the catalytic cycle. The homogeneous Ru–pincer complex was immobilized, together with the base KOH, exploiting supported liquid phase (SLP) and supported ionic liquid phase (SILP) approaches to be ideally employed in a fixed bed reactor (continuous vapor–phase process) to produce hydrogen directly available for use in fuel cells. Ionic liquids were selected in order to cope well with harsh conditions required for the catalytic cycle. Thus, tributylmethylphosphonium cation motif was coupled with methylsulfate $[CH_3OSO_3]^-$ (hydrophilic) and bis (trifluoromethylsulfonyl) imide $[NTf_2]^-$ (hydrophobic) counterions.

The surface coated catalytic material and KOH with both SLP and SILP approaches showed lower catalytic activity, but good selectivity if compared with the homogeneous counterpart at 130–170 °C and ambient pressure. Reactivity and characterization studies (variations of catalyst composition, liquid phase, base and catalyst loading) as well as process parameters (temperature, flow rate) allowed to rationalize parameters vs. supports and porosity identifying alumina and titania as the best supports. Although in the best conditions (optimum Ru–loading around 50 μmol Ru $g_{support}^{-1}$) no deactivation occurred during 70 h time on stream and ionic liquid coated support showed double activity, the overall system is affected by short term stability. Although promising in terms of concept, this approach requires improvement in order to be suitable for competitive applications.

More promising is the work developed by Inagaki and co-workers on the immobilization of the anionic bipyridonate complex **Ir 13** on periodic mesoporous organisilica also employed as molecular catalysts vapour phase flow reactions.[157] The first advantage of the heterogenized system consists in preventing catalyst deactivation due to CO_2 generation through the interconversion of **Ir 13** in its neutral **Ir 13-H** form in acidic medium (Scheme 4). This co–product is removed from the catalyst bed in the vapor–phase flow reactor, allowing the continuous generation of hydrogen without the addition of a base.

The solid support consists of periodic mesoporous organosilica (PMO) containing a chelating ligand in the framework, to form novel single–site heterogeneous catalysts. Continuous hydrogen production from a methanol–water mixture is achieved at low temperature (100 °C) without the addition of a base. The catalytic activity toward low–temperature methanol steam reforming is improved if compared with conventional impregnation and surface–grafting approaches.

Interestingly, **Ir 13-PMO** demonstrated a high catalytic activity in the vapor–phase reaction [maximum H_2 generation rate = 6.35 mmol h^{-1} g^{-1}, turnover number for 6 h (TON_{6h}) = 178.2], as evident from the continuous generation of hydrogen for at least 10 h even in the absence of a base. On the other hand, the yield of hydrogen in the liquid–phase reaction was remarkably low ($TON_{6\,h}$ = 10.5) in the presence of homogeneous **Ir 13** catalyst without base. Indeed, the immobilization positively affects the stability of the catalyst due to the removal of CO_2 while it is generated, avoiding a detrimental pH decrease. A range of characterizations including ^{13}C CP MAS NMR, X-ray absorption, fine structure (XAFS), XRD, N_2 adsorption/desorption isotherms, ^{29}Si DD MAS NMR spectroscopy, TEM, ICP–AES, and high–angle annular dark–field scanning transmission electron microscopy confirmed that the anionic **Ir 13** structure on the pore surface is maintained and the immobilized complex is not converted to the neutral **Ir 13-H** thus favouring the methanol steam reforming at low temperature and without base and enabling continuous hydrogen production over a period of 24 h with yield up to 99 % of CO free H_2.

© 2024 The Author(s). ChemCatChem published by Wiley-VCH GmbH

18673899, 2024, 17, Downloaded from https://chemistry-europe.onlinelibrary.wiley.com/doi/10.1002/cctc.202400393 by CochraneItalia, Wiley Online Library on [25/03/2025]. See the Terms and Conditions (https://onlinelibrary.wiley.com/terms-and-conditions) on Wiley Online Library for rules of use; OA articles are governed by the applicable Creative Commons License

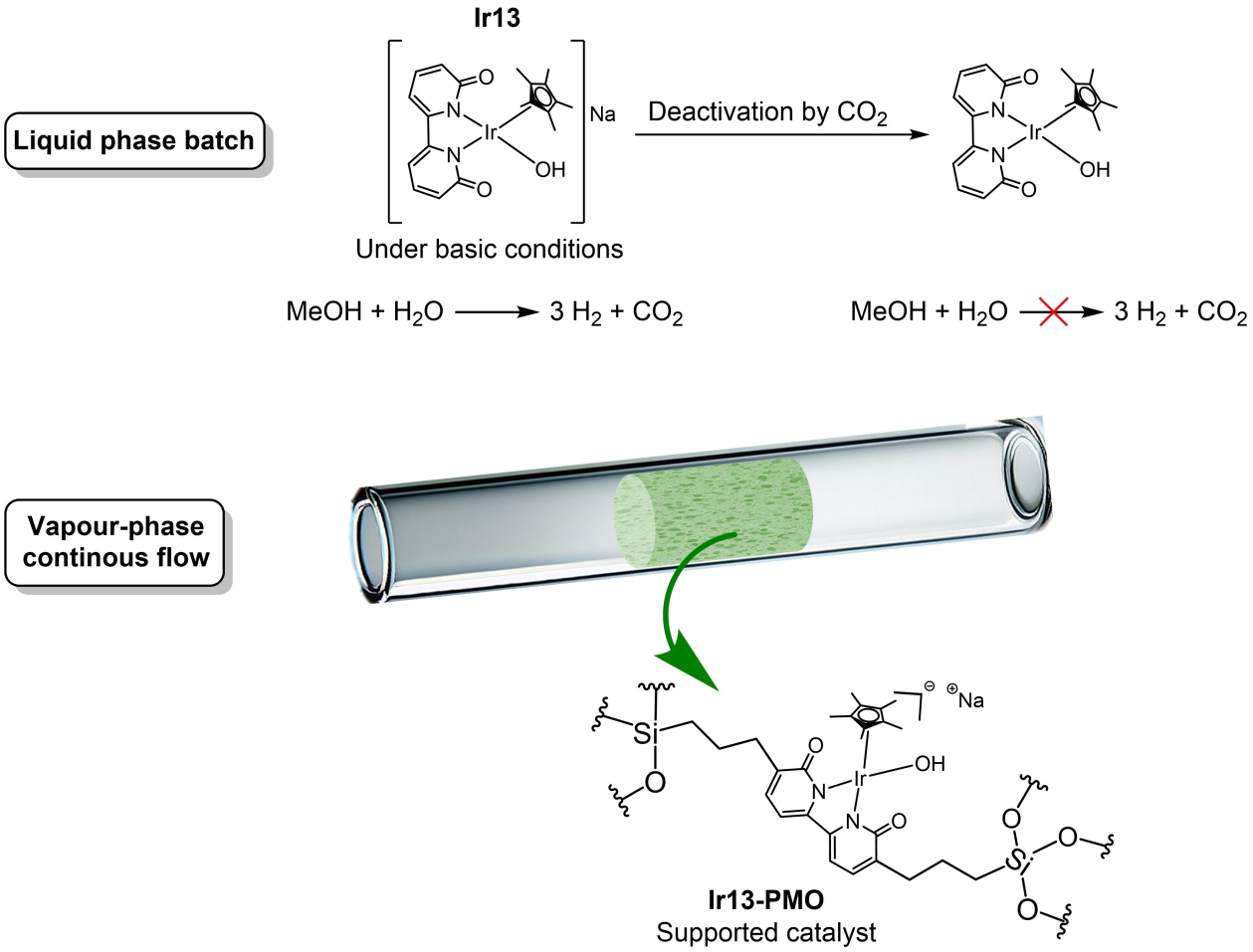

Scheme 4. Vapour phase continuos flow methanol APR promoted by **Ir 13** complex immobilized on periodic mesoporous organisilica.[157]

The same system was also tested in the dehydrogenation of ethanol/water to hydrogen and acetic acid (maximum rate of hydrogen production and $TON_{6\,h}$ were 1.89 mmol h^{-1} g^{-1} and 51.9 respectively, H_2 yield 1.9%) and 2-propanol to hydrogen and acetone (maximum rate of hydrogen production and $TON_{6\,h}$ were 13.7 mmol h^{-1} g^{-1} and 380.3, respectively, H_2 yield 47%) with a rate of hydrogen production that resulted unvaried for 6 h.

The main outcome of this work is the applicability of immobilized molecular catalysts in vapor–phase flow reactions. It provides a new direction for low–temperature vapor–phase reaction systems which could became good candidates in the development of novel catalytic processes for fuel and bulk chemical synthesis.

Acceptorless dehydrogenation of ethanol to ethylacetate or acetic acid, also declined as bio–ethanol obtained from biomass, reached its maximum interest between 2010 and 2015 as documented by the work of Beller and co-workers and others.[158–161] More recently Ru(II) complexes bearing tridentate Schiff–base ligands were employed to produce hydrogen and ethylacetate from ethanol with similar efficiency as the previously reported complexes.[162]

2.3. Hydrogen Production from Polyols: 1,4-butanediol, Ethylen Glycol (EG), Sorbitol and Glycerol

Fujita and co-workers explored the effectiveness of iridium complex **Ir 13** provided with dihydroxy bipyridine ligands in dehydrogenation of butanediol as LOHC in a reversible hydrogen storage system based in 1,4-butanediol and γ-butyrolactone.[163] Quantitative yield of H_2 was obtained with a 0.1 mol% of catalyst loading in 20 h (Scheme 5). Furthermore, the reaction performed well also in neat substrate (0.5 mol% catalyst) with an almost complete conversion of 15 mmol of 1,4-butanediol to γ-butyrolactone and a 99% yield of hydrogen.

The reverse reaction was also carried out under neat conditions and triethylamine, with a theoretical hydrogen storage capacity of 4.4 wt%. Although limited in the overall hydrogen storage capacity this reaction is an important example of LOHC applicable at low temperatures.

Ethylen glycol (EG), a large scale product with application in automotive and polyester industries,[164] is a subtrate of large interest within the framework of hydrogen storage liquid materials due to its hydrogen storage capacity of 6.5 wt%, carbon neutrality and its wide accessibility as a bio–derived feedstock.[165–168] Recent advances involved the use of acridine

© 2024 The Author(s). ChemCatChem published by Wiley-VCH GmbH

18673899, 2024, 17, Downloaded from https://chemistry-europe.onlinelibrary.wiley.com/doi/10.1002/cctc.202400393 by CochraneItalia, Wiley Online Library on [25/03/2025]. See the Terms and Conditions (https://onlinelibrary.wiley.com/terms-and-conditions) on Wiley Online Library for rules of use; OA articles are governed by the applicable Creative Commons License

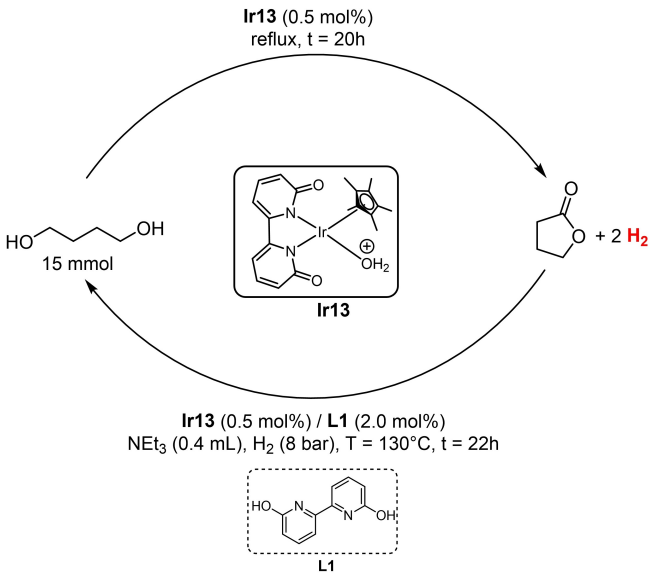

Scheme 5. 1,4-butanediol/γ-butyrolactone system for the reversible hydrogen storage in alcohol based LOHC.[163]

based PNP ruthenium complexes **Ru 17** (previously employed by Milstein and co-workers in the dehydrogenation of methanol) as a system capable to circumvent some intrinsic drawbacks of EG dehydrogenation such as catalyst poisoning by CO and chelation and formation of unwanted cyclic products resulting in lower H_2 production.[169] EG conversion of up to 94% to produce 54 mL of hydrogen gas in 72 h was obtained with 1 mol% **Ru 17**, 1 mol% KOtBu, 2.0 mmol ethylene glycol in toluene/DME (1.0 mL/1.0 mL) at 150 °C. As reported in Scheme 6 the reaction also produces hydroxyethyl glycolate (HEG) (33%), and oligoesters (theoretical hydrogen storage capacity of 6.5 wt%). Upon dearomatization of the acridine complex to **Ru 4** the reaction proceeds in the absence of base as well as in neat EG at a reduced pressure (95 mbar, 35.9 mmol EG, 2 mL, 150 °C, toward 94% conversion of EG in 7 days). The latter catalyst also promotes the reverse reaction to EG in good yield (92%) under the conditions reported in Scheme 6.

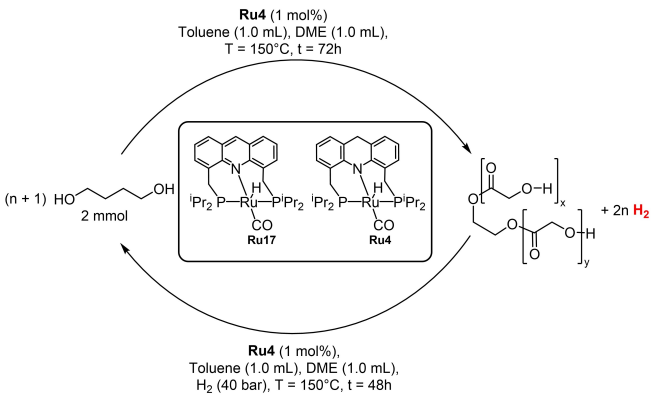

Scheme 6. EG/Oligoester LOHC system for reversible hydrogen storage.[169]

The same authors reported an important advancement in the field of aqueous reforming of EG achieving the selective production of glycolic acid in up to 91% yield and pure H_2 gas (up to 223 mL) under mild conditions (EG 5 mmol, KOH 25 mmol, H_2O/THF, 115 °C, 48 h, 0.5 mol% of best catalyst – **Ru 18** – Scheme 7), without CO_2 or CO emissions and with no need of additional organic solvents, thus providing a more atom economical, environmentally friendly and sustainable protocol. Furthermore, the reaction can be performed on a large scale of 30 mmol of EG. The reaction employed at its best a pincer ruthenium complex with PNNH non-innocent ligand.[170] Interest in the production of glycolic acid with easier and more sustainable approaches is motivated by its application in skin care, adhesives and polymers for the textile industry,[171] and due to the fact that it is usually synthesized by multiple synthetic steps associated with stoichiometric amount of waste.[172–174]

The scalability of the process was also established with a catalyst loading of 0.1 mol%, 30 mmol of EG were converted at 921 mL of hydrogen (64% yield) in 120 h. Catalyst recycling showed that the catalyst is not exhaust, but works at a lower rate. In depth computational and experimental studies allowed to depict a proposal for the mechanism reported in Scheme 8. Unravelling the non-innocent catalyst behaviour is of great importance in order to pave the way for the rational design of more active and more stable catalysts.

Promising results were recently obtained with a NNN–Ru (**Ru 19** 0.01 mol%–5 mol%) bifunctional catalyst (TON up to 25225).[175] The system produces more than two equivalent of hydrogen (optimized conditions: EG (2.503 mmol), KOH (6.25 mmol), in tBuOH at 100 °C for 2 h) and a glycolic acid yield up to 94% in a solvent free medium. Furthermore, scale up operations yielded 1230 mL of pure hydrogen. Reactivity studies were aimed to propose the catalytic mechanism depicted in Scheme 9.

Further expanding the scope of the reaction to organic transformation with the production of hydrogen as a co–product, vicinal glycols (readily available feedstock) are prone to be transformed exploiting acceptorless dehydrogenation by a PNP pincer manganese catalyst similar to **Mn 6** into value–added α-hydroxycarboxylic acids (molecule useful for biodegradable polymers).[176]

Although reforming of aqueous ethylene glycol to produce hydrogen is definitely of great interest,[177] reports are scarce

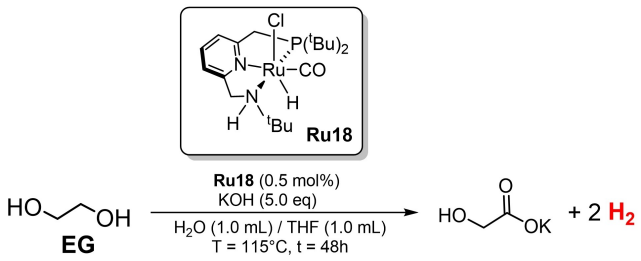

Scheme 7. Acceptorless dehydrogenation of EG to Glycolic acid catalyzed by **Ru 18**.[172]

© 2024 The Author(s). ChemCatChem published by Wiley-VCH GmbH

18673899, 2024, 17, Downloaded from https://chemistry-europe.onlinelibrary.wiley.com/doi/10.1002/cctc.202400393 by CochraneItalia, Wiley Online Library on [25/03/2025]. See the Terms and Conditions (https://onlinelibrary.wiley.com/terms-and-conditions) on Wiley Online Library for rules of use; OA articles are governed by the applicable Creative Commons License

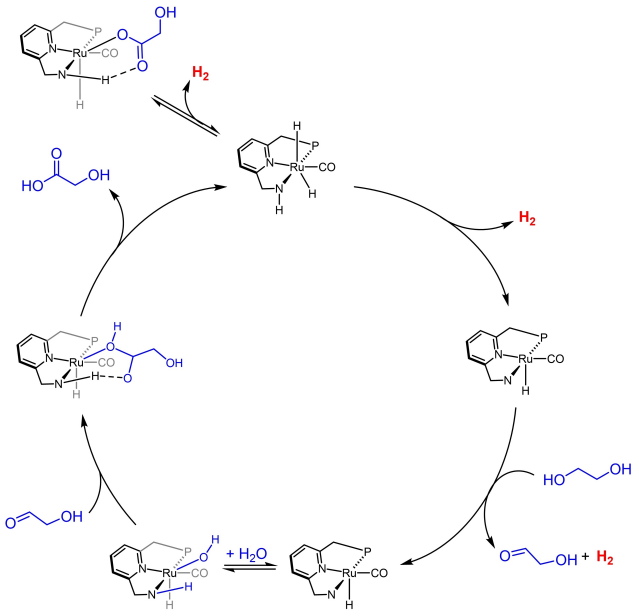

Scheme 8. Proposed catalytic cycle for the acceptorless dehydrogenation of EG to glycolic acid catalyzed by **Ru 18**.[172]

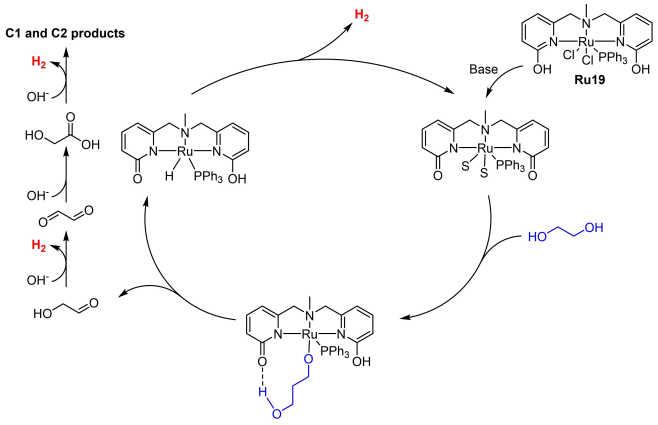

Scheme 9. Proposed reaction mechanism for the reforming of EG catalyzed by **Ru 19**.[175]

and quite recent. Selectivity and yields accomplished in the last few years make this substrate a very promising bio–derived feedstock within the framework of low temperature homogeneous processes. The knowledge for the design of new competitive catalytic systems is now available, together with the need of a deeper understanding of the reaction mechanism for future perspective in commercial applications.

Even fewer work has been devoted to renewable hydrogen production from biomass derived sorbitol It was studied for the first time by Beller and co-workers (Ru–MACHO (**Ru 8**) complex–TOF 765 h^{-1})[178] and by the Crabtree group (Ir–NHC complex (**Ir 12**) – TON of 280 and low yield).[179] Later on Tu et al., taking inspiration from the work of Crabtree, developed 3D porous self–supported NHC–iridium coordination polymers which function as recyclable solid molecular catalysts for dehydrogenation of bio–polyols to lactic acid. These systems showed excellent activity and selectivity and a synergistic participation of hydroxide anions with Ba^{2+} cations. At the same time some side reactions are avoided by adding methanol.[180] Best efficiency in pure homogeneous conditions was then obtained in 2023 by Daw and co-workers who explored metal–ligand cooperation and the effect of hydrogen–bonding on the secondary–coordination–sphere of the bifunctional NNN–Ru system **Ru 19** bearing protic arms. An interaction for the appropriate substrate orientation at the active centre was also defined reaching a maximum turnover number of 35359 (reaction conditions: **Ru 19** (1 mol %), KOH (2.5 equiv w.r.t. sorbitol), sorbitol (0.503 mmol), 150 °C, 2 mL of diglyme/water (9:1), 24 h. The catalyst was found to have a slow deactivation over seven reaction cycles. The mechanism proposed is similar to the one reported for EG (see Scheme 9 above).[181] Nevertheless this behaviour demonstrates that the chemistry of EG can be transferred to sorbitol reactivity and vice versa for future development in the field.

Recent results on the acceptorless dehydrogenation of glycerol show that Ir–NHC complexes also play a prominent role in H_2 production from bio–derived polyalcohols. Bimetallic iridium complexes involving triscarbene ligands led to the production of hydrogen and lactate with high TON (3240000) and TOF (162000 h^{-1}).[182]

A recent report underlines that the development of heterogenization strategies have come under the magnifying glass due to the urgence, once obtained efficient molecular catalysts, to increase their stability and recyclability. Stavila and co-workers[183] reported two methods for the heterogenization of commercially available ruthenium complexes as Milstein Acridine Catalyst (**Ru 4**) and Ru–MACHO (**Ru 8**) active in the dehydrogenation of EG and 1,2–propandiol (1,2–PDO). Interestingly the supported catalysts, obtained following two different synthetic pathway useful for both the catalysts (silica mounting and self–polymerization depicted in Scheme 10 for Ru–MACHO) maintain the catalytic activity (up to 81 % conversion and 99 % selectivity). In the case of **Ru 8** polymer catalyst the system is stable and effective for at least five reaction cycles. This catalyst is claimed as the first heterogenized system for the reversible catalytic dehydrogenation of polyols, which was previously developed only in homogeneous phase.

The heterogenized catalyst has been successfully recycled under the following reaction conditions: neat EG (1.000 g, 16.11 mmol), KOtBu (2.0 mg, 0.018 mmol), **Ru 8-Poly** (12.0 mg, 0.00843 mmol), 144–155 °C.

Such advances, with particular emphasis to the immobilization protocol and relative application approaches to heterogenized molecular catalysis for the production of renewable energy from polyol LOHCs, are widening the scope of stable molecular single site active species and their recyclability, an important aspect to reduce the boundaries between heterogeneous and molecular catalysts in terms of potential application to bulk processes.

© 2024 The Author(s). ChemCatChem published by Wiley-VCH GmbH

18673899, 2024, 17, Downloaded from https://chemistry-europe.onlinelibrary.wiley.com/doi/10.1002/cctc.202400393 by CochraneItalia, Wiley Online Library on [25/03/2025]. See the Terms and Conditions (https://onlinelibrary.wiley.com/terms-and-conditions) on Wiley Online Library for rules of use; OA articles are governed by the applicable Creative Commons License

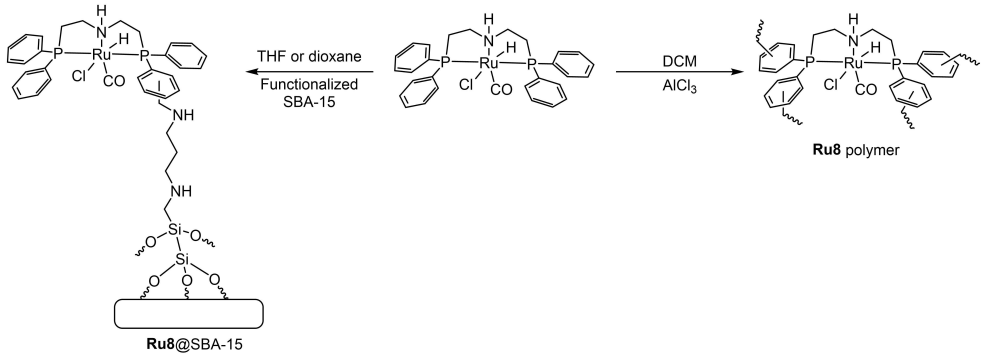

Scheme 10. The two synthetic pathways employed for the heterogenization of Ru–MACHO (**Ru 8**).[183]

2.4. Hydrogen Production from: Carbohydrates, Cellulose and Hemicellulose

Carbohydrates constitute one of the major components of plant biomass and represent an abundant and renewable feedstock for achieving platform chemicals. Among them, monosaccharides of five and six carbon rings are the basic units of cellulose and hemicellulose.[184] Increasing the feedstock complexity and moving toward sugars, only a limited number of reports involving metal–based homogeneous catalysis can be found in literature.[185] However, it is globally recognized that the full transition to a hydrogen society can be realized only with the development of effective ways to produce hydrogen via renewable resources such as biomass.[186,187]

Although important contributions on hydrogen generation from biomass have been made by means of gasification, reforming in supercritical water, enzyme fermentation and aqueous–phase reforming by heterogeneous catalysts,[145] all these approaches exhibit main limitations.

Both gasification (800–1300 °C) and reforming in supercritical water (500–700 °C, 300 bar) of biomass are energetically expensive processes and are restricted to harsh demanding process conditions.[186] On the other side, enzymatic decomposition of sugars suffers from low hydrogen production rates, long reaction times, time–consuming culturing of enzymes together with their cost and requirements of a rigorous control of the reaction parameters. Concerning heterogeneous catalysts, harsh conditions and expensive noble metals are often employed. Moreover, considerable amounts of carbon monoxide or methane are produced in the final gas mixture along with hydrogen, making downstream processing mandatory.[184,188]

As an alternative to the aforementioned high temperature processes, novel opportunities are required for potential application of biomass. The main challenges are often the poor stability and solubility of organometallic species in aqueous media, together with polysaccharides' high chemical stability, insolubility in most common solvents[189] and the control of selectivity due to the presence of many functional groups.

Nevertheless, recent developments highlighted a substantial progress of organometallic chemistry in water,[184] thus providing new opportunities for hydrogen production from sugars in mild conditions with homogeneous transition metal catalysts. All the accomplishments in this field will be described in this paragraph and the employed catalysts are summarized in Figure 5.

The aqueous phase reforming of glucose using homogeneous catalysts was introduced for the first time by Wasserscheid and co-workers in 2010,[186] who reported a seminal work on hydrogen generation accompanied by CO_2 production from glucose and cellulose in ionic liquids at 150–180 °C (Scheme 11). The compound $[(p\text{-cymene})RuCl_2]_2$ and TMEDA (tetramethylethylenediamine) as a stabilizing ligand was selected as the catalytic system since its well–known stability in dehydrogenation of isopropanol at high temperatures.[190]

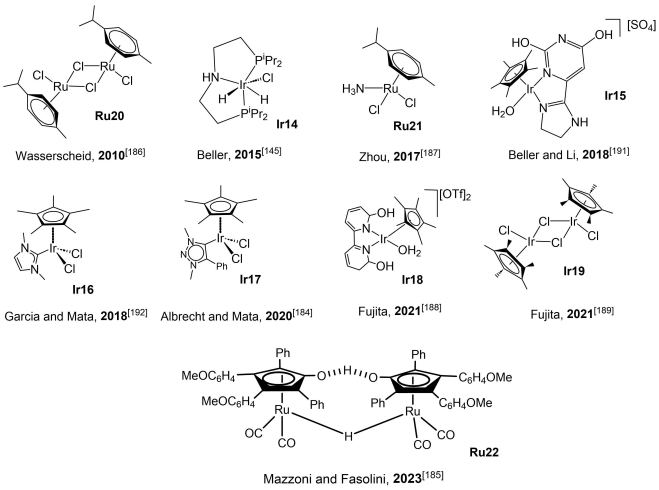

Figure 5. Catalysts for hydrogen production from carbohydrates through homogenous catalysis from 2010 to present.

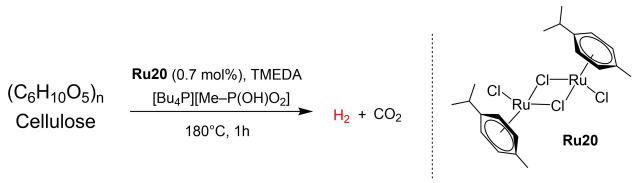

Scheme 11. Catalytic conditions mediated by **Ru 20** for hydrogen production from cellulose.[186]

© 2024 The Author(s). ChemCatChem published by Wiley-VCH GmbH

18673899, 2024, 17, Downloaded from https://chemistry-europe.onlinelibrary.wiley.com/doi/10.1002/cctc.202400393 by CochraneItalia, Wiley Online Library on [25/03/2025]. See the Terms and Conditions (https://onlinelibrary.wiley.com/terms-and-conditions) on Wiley Online Library for rules of use; OA articles are governed by the applicable Creative Commons License

Apart from hydrogen, the only detectable gas product was CO_2, and no traces of carbon monoxide, methane or other alkanes were detected, showing how hydrogenation side reactions are effectively suppressed in ionic liquids, which are also able to perfectly dissolve the substrates over the reaction course. This was a crucial point in the successful application of heterogeneous catalysed aqueous phase reforming for glucose that is now overcome in homogeneous conditions.

Among the tested solvents, tetrabutylphosphonium methylphosphonate ([Bu_4P][Me–P(OH)O_2]) resulted the most stable ionic liquid for glucose dehydrogenation. Interestingly, the presence of water in traces in the system displayed a beneficial role in the reaction efficiency. The optimized protocol was then expanded to pure cellulose which, surprisingly, was directly converted into hydrogen in the ionic **Ru 20** solution without requiring any pre– and post– treatment. Moreover, results in hydrogen evolution were in line with those obtained in the case of glucose.

Mechanistic investigations were performed in order to elucidate the catalytic route *via* ^{13}C-NMR spectroscopy using fully ^{13}C-labeled glucose. From NMR experiments, formic acid was undoubtedly detected, arising from the thermal decomposition of glucose, and immediately converted into hydrogen and CO_2 (1:1 ratio) in the presence of **Ru 20**. Accordingly, a mechanism was proposed, involving a sequence of glucose de–hydration/re–hydration (Scheme 12). In the first step, glucose was dehydrated to 5-hydroxymethylfurfural (HMF), which is then transformed into levulinic and formic acid (second step). Thus, with lower water content in the system, its formation by re-hydration proceeds slower. The same pathway is expected also for cellulose, even if it can be assumed that the thermal depolymerization of cellulose into glucose is a pre-requisite for hydrogen production.

From the mechanism elucidation, it is deduced that a mole of formic acid (and consequently a mole of gaseous hydrogen) is produced per mole of glucose. Accordingly, from the best experimental conditions, yield of hydrogen after 1 hour resulted 31.2% and 12.0% with glucose and cellulose as substrate, respectively.

The extensive work by Wasserscheid paved the way for the following advances in homogeneous catalytic hydrogen production from renewable feedstocks, reporting for the first time a one–step catalytic production of hydrogen from glucose and, more importantly, from cellulose without pre–treatment in mild conditions. In particular, the proposed ionic liquid based catalytic system was feasible and stable up to 48 h at 180 °C, allowing up to six consecutive glucose dehydrogenation reactions.

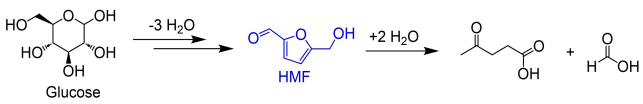

Scheme 12. Proposed mechanism of de–hydration/re–hydration of D-glucose.[186]

Nevertheless, some issues have to be overcome, being the focus of the future studies onwards. Basically, the hydrogen yield must be substantially increased, together with the catalyst turnover numbers (TONs). In fact, an efficient system should allow the generation of more than one equivalent of H_2 per monosaccharide unit. In addition, large amounts of a non–commercial ionic liquid are required, whose purification and removal from biomaterial degradation products is complex and could hamper an extensive applicability of the process.

Beller and Li in 2015[145] took inspiration from the pioneering work of Wasserscheid,[186] describing for the first time the hydrogen production from biomass in the presence of a iridium catalyst (**Ir 14**) at relatively mild conditions (temperature < 120 °C). The authors selected L-(–)-fructose as benchmark substrate and explored diglyme/stoich. KOH as useful solvent/base combination able to solubilize both the hydrophilic starting material and the transition metal catalyst at 95 °C, after an initial burst at 127 °C (Scheme 13a).

A screening of different Ru–based pincer–type catalysts revealed promising, even if the outcome of the process outperformed when ruthenium was replaced with an iridium–based catalyst and KOH with sodium hydroxide (1.5 equiv). The best reactivity resulted in a TOF of 5559 h^{-1} after 2 h. Here, conversion of 2.0% (based on 6 mol of H_2 produced per mol of monosaccharide) was obtained, which was increased to 2.6% upon increasing the catalyst loading from 10 to 500 ppm. Not surprisingly, when the temperature was raised to 140 °C, hydrogen conversion reached a 3.4% value, while variations in the amount of substrate did not lead to a significant outcome.

The concomitant formation of carbon dioxide, calculated from both gaseous and solution phase analysis, proved a C–C bond cleavage of the monosaccharide. In addition, acid hydrolysis of the reaction mixture indicated that most of the CO_2 was trapped in solution as (bi)carbonate. Notably, CO and CH_4 contents were also detected.

With the optimized conditions, D-(+)-glucose and D-(+)-cellobiose were also tested (Scheme 13a), acting as examples of a different monosaccharide and a disaccharide, respectively. Both sugars showed good efficiency, comparable to fructose (TOF after 2 h: 4329 h^{-1} for glucose and 5359 h^{-1} for cellobiose).

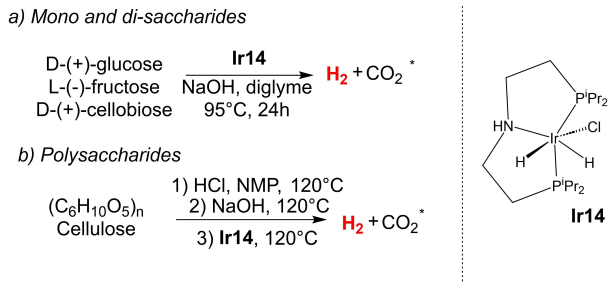

Scheme 13. a) Catalytic conditions mediated by **Ir 14** for hydrogen production from mono– and disaccharides; b) Catalytic conditions mediated by **Ir 14** for hydrogen production from cellulose.[145] * In the cases a) and b) here described CO and CH_4 have been also detected in the gas phase.

© 2024 The Author(s). ChemCatChem published by Wiley-VCH GmbH

18673899, 2024, 17, Downloaded from https://chemistry-europe.onlinelibrary.wiley.com/doi/10.1002/cctc.202400393 by CochraneItalia, Wiley Online Library on [25/03/2025]. See the Terms and Conditions (https://onlinelibrary.wiley.com/terms-and-conditions) on Wiley Online Library for rules of use; OA articles are governed by the applicable Creative Commons License

Mechanistic insights on H_2 production from monosaccharides were attempted through NMR analysis of fructose and glucose reaction mixtures in the presence and absence of catalyst. As a result, sodium formate and other carboxylic acid salts were revealed as intermediates before addition of the catalyst, with no substantial differences between the two analysed substrates.

The authors also explored more challenging carbohydrates (cellulose and lignocellulose) as source of hydrogen from biomass (Scheme 13b). However, the first attempts demonstrated how a pretreatment consisting of cellulose hydrolysis into glucose/cellobiose was needed to generate hydrogen with satisfactory TON values, due to the substrate low solubility. After a systematic study, the best conditions were found in firstly dissolving cellulose in aqueous *N*-methylpyrrolidone (NMP) and HCl at 120 °C. The hydrolytic pretreatment was followed by neutralization with sodium hydroxide and addition of the iridium–based pincer complex to perform hydrogen production, maintaining the temperature at 120 °C (TON_{2h} : 6285).

The same protocol was finally applied to lignin; feedstocks from pulp and second–year bamboo were investigated displaying good activities under optimized conditions, together with cellulose acetate fibers.

The detection of only partial amounts of glucose and reducing sugars after the hydrolysis step of polysaccharides suggested that hydrogen production mainly takes place from the corresponding oligomers, which displayed an increased solubility but a similar reactivity than the mono– and disaccharides.

Despite the advantages of this novel process such as mild reaction conditions, low amounts of catalyst required and wide applicability of the system also to demanding polysaccharides, the yields of hydrogen remain poor, and no mechanistic details are described, since only the gas phase of the reaction mixtures was analysed.

A couple of years later, Zhou and coworkers[187] developed a process for glucose dehydrogenation at temperatures below 100 °C with a series of water–soluble organo Ru, Rh, and Ir catalysts, using water as reaction medium and sulphuric acid as additive.

Hydrogen generation from glucose hydrate was found to be strongly dependent on the metal complex and its organic ligands, with [(*p*-cymene) $Ru(NH_3)$] Cl_2 (**Ru 21**) displaying the best results with a maximum TOF value of up to 719 h^{-1} ($TOF_{1\,h}$: 270 h^{-1}).

A correlation between the gas volume and the reaction time for the glucose dehydrogenation was highlighted, with a rapid increase in the first 10 minutes, followed by a rate decrease. A deactivation of the catalyst along time was anyway excluded. The components of the gaseous phase arising from glucose decomposition were analysed, revealing the detection of only CO_2 apart from hydrogen, which gradually increased over time. No traces of carbon monoxide were detected in this case.

A careful screening of the reaction conditions unveiled a linear influence of the reaction temperature on hydrogen evolution and an effect of the increase in the initial glucose concentration, with a maximum reached at 0.66 mol L^{-1}, followed by a rapid drop at higher concentration values. Finally, also the pH of the solution disclosed a relevant effect on the production of H_2, resulting in an increase in hydrogen evolution at pH decreasing, with a maximum value detected at pH = 0.5.

By analysing *via* NMR spectroscopy the liquid reaction phase, the intermediates of the process were detected. Accordingly, the authors proposed a mechanism (Scheme 14) comprising the "aldehyde–water shift" (AWS) reaction as a first step, in which H_2 is generated from glucose to give the carboxylic acid as oxidised product with H_2O as terminal oxidant. Then, in the rate determining step, the D-glucose acid occurs decarboxylation due to its structural instability, leading to formic acid formation. Finally, the ruthenium complex, prone to C–C cleavage, catalyses the immediate decomposition of formic acid in H_2 and CO_2. As a result, the catalyst activity is correlated to the acidity – as a free H is required to close the catalytic cycle – and only strong acidic conditions allow the hydrogen production process (whereas basic conditions are detrimental for the reaction).

Despite the advantages of low temperatures and stability of **Ru 21** in the aqueous media, the strong acidity required for the proposed system translates in complicate industrial possible applications due to high corrosivity.

After their preliminary work dated back to 2015,[145] the group of Beller and Li further expanded the panorama of homogenous catalytic–hydrogen production from biomass, reporting in 2018[191] a one–pot, two–step strategy to obtain molecular hydrogen from various renewable non–food–related feedstocks. Considering formic acid (FA) as a suitable intermediate in the decomposition of biomass, the authors designed a process in which the major components of renewable feedstocks were transformed *via* an oxidative catalysis in formic acid. This is followed by a direct H_2 production without purification under mild conditions through a reductive catalysis mediated by iridium complexes.

More specifically, a first hydrolysis–oxidation of cellulose and hemicellulose in biomass furnished formic acid. The oxidation step with D-glucose as a model unit of cellulose was performed with O_2 (3.0 MPa) in the presence of 6 mol % sodium metavanadate in 0.7 wt % H_2SO_4 solution. In order to obtain full miscibility of all compounds in the aqueous phase, 1 v % of dimethylsulfoxide (DMSO) as a co–solvent was added. Subsequently, the catalytic amount of acid was neutralized and H_2 was straight produced by the addition of a ppm–scale (208) homogeneous **Ir 15**, stable in the aqueous mixture, at 90 °C. The unwanted side products CO and CH_4 were detected only in negligible amounts.

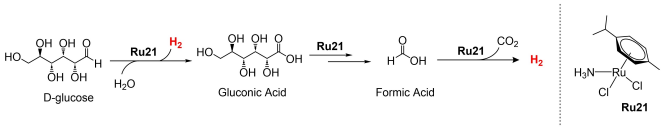

Scheme 14. Proposed mechanism of hydrogen production from glucose *via* intermediate formic acid.[187]

© 2024 The Author(s). ChemCatChem published by Wiley-VCH GmbH

18673899, 2024, 17, Downloaded from https://chemistry-europe.onlinelibrary.wiley.com/doi/10.1002/cctc.202400393 by CochraneItalia, Wiley Online Library on [25/03/2025]. See the Terms and Conditions (https://onlinelibrary.wiley.com/terms-and-conditions) on Wiley Online Library for rules of use; OA articles are governed by the applicable Creative Commons License

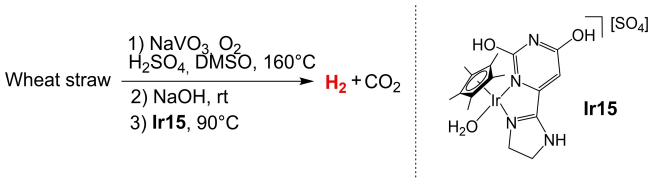

Scheme 15. Catalytic conditions mediated by **Ir 15** for hydrogen production from wheat straw.[191]

The process was then replicated for cellulose and wheat straw feedstocks (Scheme 15). Notably, the latter was able to quantitatively generate formic acid on a gram–scale in the presence of 4 mol % $NaVO_3$ within 3 hours.

In these cases, FA and H_2 yields were calculated on the amount of carbon in the polysaccharides (cellulose and hemicellulose). After the first hydrolysis–oxidation step, the hydrogen production from the obtained FA mixture resulted more struggling, with low TONs and high levels of detected side product CO. Only the choice of the right iridium catalyst among a wide panel of candidates allowed to obtain high H_2 yields in short times.

Ir 15 displayed a high dehydrogenation activity in aqueous FA, which was further increased when its loading was decreased to 69 ppm and the pH of the first step was adjusted to 2.25. In these best conditions, H_2 yield reached values of 95 % in less than 30 minutes (TON = 13,6). Prompted by this unexpected productivity, other carbohydrate–based wastes (corn and rice straw, reed, bagasse, bamboo sawdust, etc..) were tested under these optimized conditions, showing on average very good H_2 yields (68–95 %) with contextual low amounts of detected CO (6–13 ppm) and CH_4 (< 2 ppm).

From the liquid phase investigation of the hydrolysis–oxidation mixture and a series of kinetic experiments, the authors depicted a possible mechanism of the H_2 production from biomass–derived FA, arising in turn from the hydrolysis–oxidation of biomass (Scheme 16). The coordination equilibrium between FA and **Ir 15** or the corresponding active complex occurs before the rate–limiting step. In particular, **Ir 15** is readily converted into its active species **A** that is in equilibrium with **B** after coordination of formic acid. At this point, **B** undergoes decarboxylation to give iridium hydride **C**, which is in turn protonated to intermediate **D** that regenerates the active complex **A** after H_2 releasing.

This work was able to overcome two major challenges common in the biomass treatment: the avoidance of large amounts of expensive organic solvents while maintaining an efficient hydrogen production (yields up to 95 %), and the scaling–up to gram scale reaction, which is rarely reported, keeping the catalyst use at a ppm scale in mild conditions. It is worth noting that an attempt to recycle the oxidative vanadium catalyst and the reductive **Ir 15** was performed. In fact, the freeze–dried residue from the wheat straw experiment containing vanadium and iridium complexes was added to the first and the second step, respectively, obtaining 61 % FA and 19 % H_2 yield. However, using the described system conditions, the reaction required a toxic reagent and a high–pressure oxygen atmosphere. Moreover, preparation of the catalyst was not straightforward, and the multi–step procedure could be considered problematic from an economy and handling point of view. Accordingly, the accomplishment of hydrogen through a simple one–step procedure from biomass is desired in order to save resources and improve feasibility.[189]

On the same year, Garcia and Mata[192] reported an alternative process for the transformation of glucose into gluconic acid using homogeneous Cp*Ir complexes with imidazole–based *N*-heterocyclic carbene (NHC) ligands. In the described transformation, the iridium complex was added to a solution of glucose using water as a solvent under mild reaction conditions (reflux temperature).

Through a preliminary monitoring of the reaction outcome by ESI–MS, the oxidation of glucose into gluconic acid resulted selective without additives with catalyst precursor **Ir 16**. In fact,

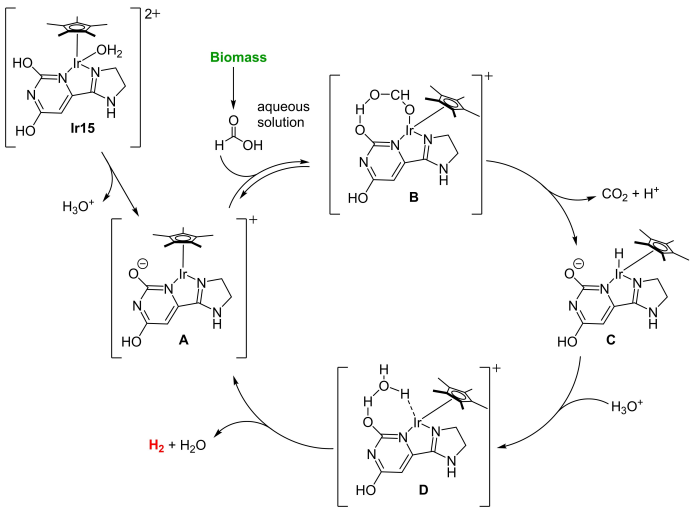

Scheme 16. Proposed mechanism of hydrogen production from biomass-derived formic acid catalysed by **Ir 15**.[191]

© 2024 The Author(s). ChemCatChem published by Wiley-VCH GmbH

18673899, 2024, 17, Downloaded from https://chemistry-europe.onlinelibrary.wiley.com/doi/10.1002/cctc.202400393 by CochraneItalia, Wiley Online Library on [25/03/2025]. See the Terms and Conditions (https://onlinelibrary.wiley.com/terms-and-conditions) on Wiley Online Library for rules of use; OA articles are governed by the applicable Creative Commons License

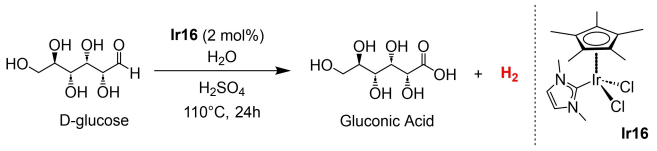

Scheme 17. Catalytic conditions mediated by **Ir 16** for hydrogen production from D-glucose in water.[192]

no formation of potential acids and ketoacids deriving from glucose was detected. Also in this case, glucose dehydrogenation was found to be dependent to pH variation. Whilst basic conditions led to substrate degradation and consequent lowering in gluconic acid yield, the addition of acid to the reaction media (0.25 eq. of H_2SO_4 or HCl) consistently improved the process with the same selectivity to gluconic acid (88% yield obtained after 30 min with H_2SO_4 and **Ir 16**, Scheme 17).

With the optimized conditions, the authors explored the transformation of starch, a polysaccharide constituted by glucose monomers bonded by β-glycosidic bonds, into gluconic acid, to demonstrate the applicability of the process to more challenging carbohydrate targets. However, even with stronger conditions, the reaction proceeded slowly due to a tricky hydrolysis of glycosidic bonds (50% glucose yield and 80% glucose conversion after 50 h).

In order to elucidate the general mechanism of the dehydrogenation of glucose to gluconic acid, NMR and ESI–MS analyses were implemented with density functional theory (DFT) calculations. It was demonstrated that **Ir 16** underwent an equilibrium by chloride–water ligand exchange upon dissolution in water, leading to the formation of the aqua complex $[Cp^*Ir(NHC)(H_2O)_2]^{2+}$ ($\mathbf{E}^{2+}$), whose presence is favoured in acidic conditions compared to the corresponding hydroxo species. This could exemplify the faster glucose conversion at low pH, and the presence of $\mathbf{E}^{2+}$ as the active catalyst. To start the catalytic cycle (Scheme 18), the labile H_2O ligands in complex **E** are exchanged with glucose leading to species **F** that displays a chelate arrangement through the carbonyl and the hydroxo group and was detected by ESI–MS at the initial reaction stages.

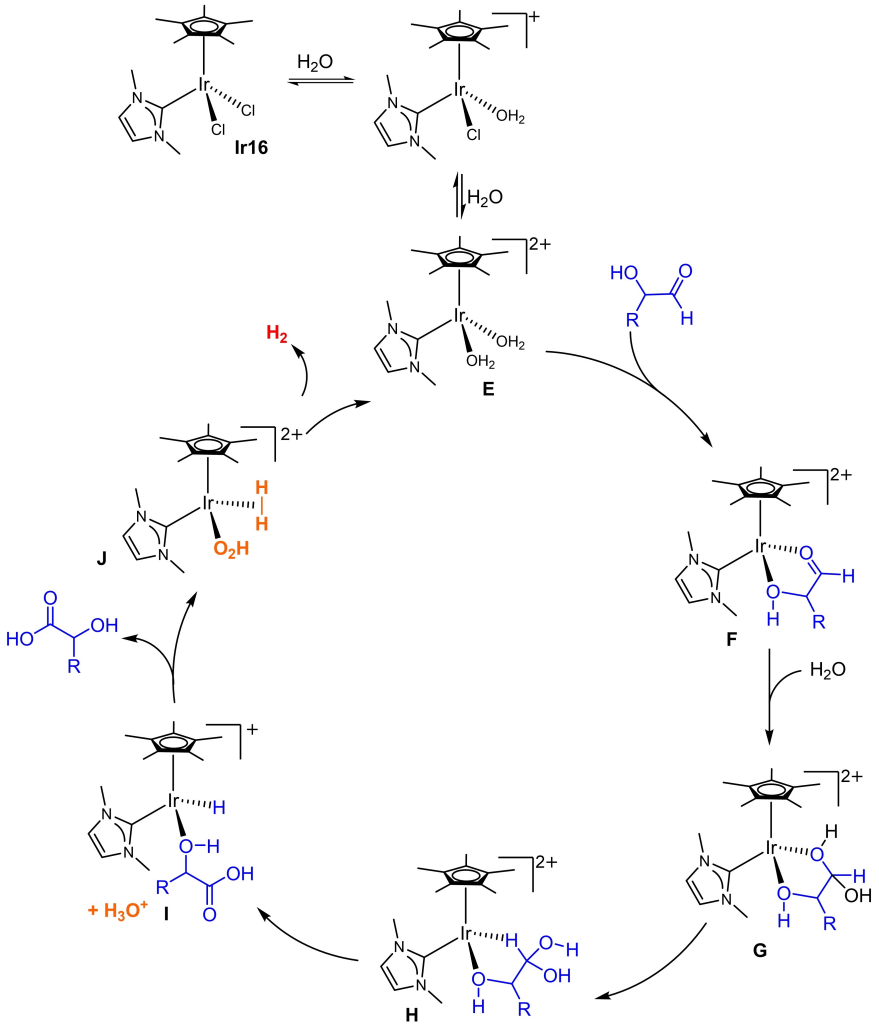

Scheme 18. Proposed mechanism of hydrogen and gluconic acid production from glucose catalyzed by **Ir 16**.[192]

© 2024 The Author(s). ChemCatChem published by Wiley-VCH GmbH

18673899, 2024, 17, Downloaded from https://chemistry-europe.onlinelibrary.wiley.com/doi/10.1002/cctc.202400393 by CochraneItalia, Wiley Online Library on [25/03/2025]. See the Terms and Conditions (https://onlinelibrary.wiley.com/terms-and-conditions) on Wiley Online Library for rules of use; OA articles are governed by the applicable Creative Commons License

Despite a considerable stability of **F** due to this cyclic arrangement, experimental attempts to isolate the corresponding crystals failed. The carbonyl group of the coordinated glucose experienced a nucleophilic attack by water for obtaining a gem–diol species **G**, which in turn rearranges to produce **H** that releases gluconic acid and a solvated proton (H_3O^+) forming the iridium hydride **I** (rate determining step). Finally, **I** is protonated, originating a dihydrogen species **J** that regenerates the catalyst by hydrogen release.

The results obtained in this work revealed an innovative dehydrogenative coupling of glucose and water with the concomitant formation of gluconic acid in a selective way and molecular hydrogen by homogeneous iridium complexes. Accordingly, a plausible mechanism was usefully formulated. However, the applicability of this methodology to transformation of biomass into added–value chemical products resulted still unrealistic, together with the drawbacks of using strong acids and relatively large amounts of catalyst (2.0 mol%) to efficiently promote the reaction.[188]

In order to overcome the limitations in the above–described preliminary work, the same authors proposed a modulation of organometallic species with suitable ligands to improve activity and contextually exclude the use of acid additives. In 2020[184] the study was extended to iridium complexes bearing triazolylidene (trz) ligands as substituents that could modulate the electronic and the steric properties of the catalytic system. Moreover, complexes containing a triazole–derived ligand resulted strongly water soluble, due to an enhanced polarity and a backbone nitrogen atom for a possible hydrogen bond.

The catalytic conversion of sugars into sugar acids was tested in the same conditions reported in 2018.[192] Also in this case glucose was entirely converted into gluconic acid without detection of related side products. Surprisingly, the newly introduced **Ir 17** did not require an acid additive (>90% conversion of glucose after 7.5 h) and resulted to not undergo decomposition upon thermal stability tests at 100 °C (Scheme 19).

The substrate scope was then expanded to other monosaccharides and a range of pentoses and hexoses were successfully converted into the corresponding sugar acids by dehydrogenation with the formation of molecular hydrogen in up to 90% yield. A mechanistic elucidation was given also in this case, again by combining NMR, ESI–MS and UV–Vis orthogonal techniques. An intermediate dicationic diiridium-hydride species **K** with molecular formula $[Cp^*(trz)Ir(\mu\text{-}H)2Ir(trz)\text{-}Cp^*]^{2+}$ was identified by NMR spectroscopy (hydride signal in the typical region at −16.8 ppm) and undoubtedly isolated by single crystal X-ray diffraction.

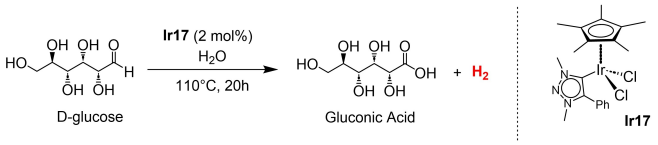

Scheme 19. Improved catalytic conditions mediated by **Ir 17** for hydrogen production from D-glucose in water.[184]

The reported mechanism (Scheme 20) is analogous to that previously reported proceeding with the formation of a gem–diol species **L** that releases a solvated proton and undergoes β-hydride elimination delivering the sugar acid product. The so obtained monohydride intermediate iridium hydride **M** is in equilibrium with the already described dimetallic complex **K**, which corresponds to the off–cycle catalyst resting state. In the final stage, **M** is protonated to intermediate **N**, which releases the proton and the metal–bound hydride as H_2, regenerating the active diaqua–catalytic species **O**. The protonation step in intermediate **N** is thought to be accelerated by the triazolylidene ligand due to the ligand basic N_2 site that could potentially enable a fast intramolecular proton shuttle from nitrogen to the iridium–bound hydride. Remarkably, such proton transfer is not feasible with complexes bearing NHC ligands and may therefore explain the need for strong acid additives, on the contrary to triazole–derived carbenes.

In this improved procedure, the conversion of sugars into sugar acids was achieved without any additional acid using triazolylidene complexes in only water as solvent. Moreover, the substrate scope was broadened to different carbohydrates that did not require purification in order to isolate the corresponding sugar acid products, due to the highly selective oxidation of the C1 position of the sugars. Applicability to polysaccharides remains an undeveloped point.

In 2021, Fujita and co-workers reported simultaneously two studies on iridium catalyst mediated- hydrogen production in water from monosaccharides[188] or from cellulose[189] feedstocks, respectively.

In the first study,[188] glucose was subjected to dehydrogenation in water under reflux conditions in the presence of a water–soluble dicationic iridium catalyst **Ir 18** (Scheme 21).

As a result, hydrogen was obtained in 76% yield after 20 h without acid or base additives with 0.2 mol% catalyst, revealing how the presence of a hydroxy group at the 6,6–position of the ligand is essential for catalytic efficiency. The yield of the process was then successfully improved to 95% by increasing the amount of the catalyst **Ir 18** to 1.0 mol%, also revealing that the gas production consisted in highly pure H_2 only.

Catalytic tests were also performed on glucose analogues carrying differently protected hydroxy groups, with the aim of clearly depicting the site where dehydrogenation reaction takes place. As already demonstrated by other previous studies,[184] hydroxy group at the 1–position is the one responsible for hydrogen production.

Other monosaccharides as D-galactose, D-mannose, and L-arabinose were then employed as substrates in the same conditions, giving the corresponding lactone structures and hydrogen gas in good yields. Only when D-fructose was used, the H_2 yield dropped due to the complicated dehydrogenation from the alcoholic moiety at 1-position.

In summary, the reaction proceeded smoothly without requiring strong acid or basic additives, despite the quite large amount of required iridium catalyst and the long reaction times.

In the meantime, the catalytic chemistry of homogeneous iridium complexes involving the hydrogen transfer and dehy-

© 2024 The Author(s). ChemCatChem published by Wiley-VCH GmbH

18673899, 2024, 17, Downloaded from https://chemistry-europe.onlinelibrary.wiley.com/doi/10.1002/cctc.202400393 by CochraneItalia, Wiley Online Library on [25/03/2025]. See the Terms and Conditions (https://onlinelibrary.wiley.com/terms-and-conditions) on Wiley Online Library for rules of use; OA articles are governed by the applicable Creative Commons License

18673899, 2024, 17, Downloaded from https://chemistry-europe.onlinelibrary.wiley.com/doi/10.1002/cctc.202400393 by CochraneItalia, Wiley Online Library on [25/03/2025]. See the Terms and Conditions (https://onlinelibrary.wiley.com/terms-and-conditions) on Wiley Online Library for rules of use; OA articles are governed by the applicable Creative Commons License

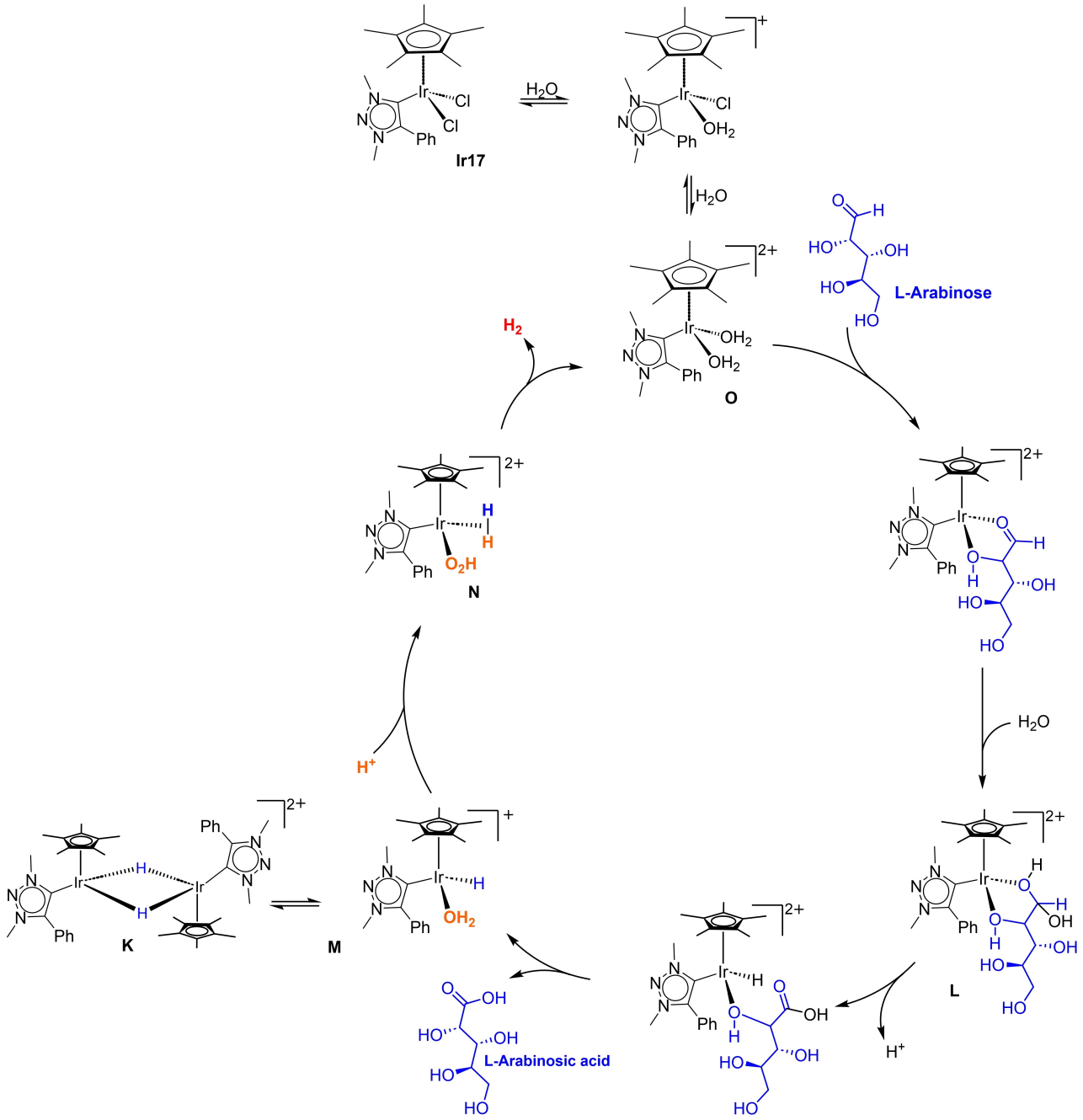

Scheme 20. Improved proposed mechanism of hydrogen and arabinosic acid production from arabinose catalysed by **Ir 17**[184]

drogenative transformation of celluloses – as polysaccharides bearing many hydroxy groups – was studied. Taking inspiration from the pioneering work by Wasserscheid,[186] Fujita *et al.* employed ionic liquids to dissolve cellulose for hydrogen production.[189] In this case the authors employed iridium–based complexes under milder reaction conditions if compared with the previously described ruthenium catalysts.

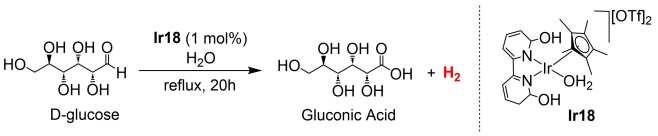

Scheme 21. Catalytic conditions mediated by **Ir 18** for hydrogen production from D-glucose in water.[188]

The potential of different catalysts was examined and an ionic liquid/water system was employed at 135 °C for 24 h (Scheme 22). Pentamethylcyclopentadienyl iridium dichloride dimer $[Cp^*IrCl_2]_2$ (**Ir 19**) outperformed among the tested candidates yielding hydrogen in 60 % yield. In order to gain pure hydrogen as the end–product, carbon dioxide, a side

© 2024 The Author(s). ChemCatChem published by Wiley-VCH GmbH

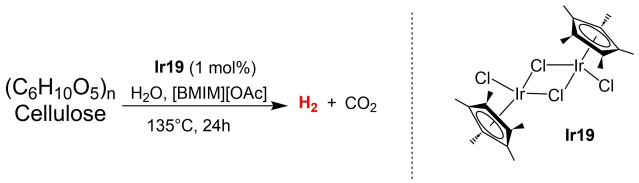

Scheme 22. Catalytic conditions mediated by **Ir 19** for hydrogen production from cellulose in ionic liquid.[189]

product of the gaseous mixture, could be trapped by passing the evolved gas through a sodium hydroxide solution.

1–butyl–3-methylimizolium acetate [BMIM][OAc] revealed to be the best solvent for the catalytic reaction, which harshly progressed in ionic liquids without acetate anions. Since also when cellobiose was used as a substrate the reaction gave satisfactory results (61 % yield), it can be stated that dehydrogenation occurs from the β-glucose component. On the other side, acetyl cellulose provided a decreased yield (37 %), confirming how the generation of hydrogen from cellulose passes through dehydrogenation of the hydroxyl moieties.

With the reported conditions, cellulose was efficiently transformed into hydrogen via a simple one–step procedure using a readily available catalyst and ionic liquid at a relatively low temperature. As an added value to the process, the produced hydrogen was straightforward exploited for an alkene hydrogenation (as a chemical process) and for generation of electricity by means of a reversible fuel cell, resulting in simple LED emission. Also in this case, reaction times were long (24 hours) and catalyst was employed at 1 mol % amount. However, the reuse of the catalyst was at least attempted by performing subsequent experiments in which cellulose and water were re–added to the mixture after completion of the first run. Unfortunately, the obtained results (29 % yield in the second run) are far away for being appealing and should be consistently improved.

Recently, our group[185] applied this kind of chemistry to ruthenium molecular complexes bearing a cyclopentadienone suitable for aromatization/dearomatization, active in several reactions within the framework of hydrogen borrowing.[193–201] Ru–based cyclopentadienone complexes were investigated in homogenous aqueous phase reforming of glucose. In particular, the commercial Shvo complex **Ru 22**, used for the first time for the hydrogen evolution from sugars, was found to be effective, combining stability and easy of handling.

The model reaction was conducted with glucose as model substrate in a DMSO/H_2O 1 : 1 medium at 150 °C for 4 hours. The presence of a co–solvent was required to favour the catalyst solubility (2 mol % loading). Interestingly, no acid or basic additives were required for preserving the catalytic performances. Monitoring the glucose APR reaction over time, the best conditions were found at 2.5 h, where the observed H_2 yield was 28.9 % (TON = 15).

The effect of the pH on the mixture was anyway investigated, but a decrease in yield was reported both in acidic and in basic conditions, with neutral environment confirming as the best. Considering that ionic liquids were successfully applied in APR of carbohydrates, as previously described, 1-butyl-3-methylimidazolium trifluoromethanesulfonate ([BMIM][TfO]) was tested in the glucose APR standard protocol. In these conditions, since hydrogen production resulted negligible, Shvo complex possibly decomposed *via* the formation of a unactive ruthenium cyclopentadienone complex **P** (Scheme 23).

The substrate scope was then expanded to fructose and arabinose as sugars, and sorbitol and glycerol as polyols stating that only arabinose was effective in hydrogen production. This proved how the structure and the functional groups of the biomass–derived compounds played a crucial role in unlocking the hydrogen production pathways. Only glucose and arabinose, bearing a terminal aldehydic group, could react with water in the "aldehyde water shift reaction" to provide hydrogen and carboxylic acids.[202] Conversely, when the reaction was attempted using formic acid as substrate, 88 % H_2 yield was detected, making this compound a possible intermediate in the catalytic cycle.

By analysing the crude reaction mixtures after extraction by NMR and FTIR techniques, a monomeric ruthenium structure containing two terminal carbonyl groups and a coordination with HMF was detected (Scheme 23), depicting a catalyst stabilization in the reaction resting state. This species displayed a higher metal carbonyl backbonding, making plausible a sigma bonding ligand on the Ru vacant site.

Moreover, through *in situ* NMR experiments, the presence of HMF arising from the dehydration of fructose after anomerization of glucose at high temperatures was confirmed. This behaviour could also explain the lower performances of fructose as starting monosaccharide, if compared to glucose. Also arabinose, which exhibited activity in the aqueous reforming above described, was found to be a reaction intermediate when glucose was used as a substrate, directly arising from this sugar with contextual co–formation of formic acid that in turn was reformed to CO_2 and H_2 by ruthenium catalysis, as previously stated. The proposed and validated mechanism hence excluded the other possible reaction pathway involving glucose decarbonylation to give carbon monoxide and then CO_2 (water gas shift reaction), affirming formic

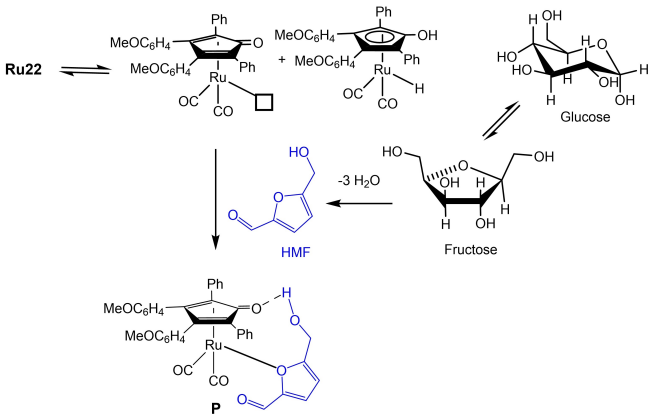

Scheme 23. Proposed catalyst **P** stabilization in the reaction resting state.[185]

© 2024 The Author(s). ChemCatChem published by Wiley-VCH GmbH

18673899, 2024, 17, Downloaded from https://chemistry-europe.onlinelibrary.wiley.com/doi/10.1002/cctc.202400393 by CochraneItalia, Wiley Online Library on [25/03/2025]. See the Terms and Conditions (https://onlinelibrary.wiley.com/terms-and-conditions) on Wiley Online Library for rules of use; OA articles are governed by the applicable Creative Commons License

acid decomposition as direct source of CO_2 production (Scheme 24). The detection of furfural and HMF in the reaction mixture corroborated this hypothesis.

As a result, the commercial Shvo complex **Ru 22** resulted effective during APR of glucose in neutral medium revealing activity similar to those reported in the literature. An extensive mechanism investigation discriminated between the two possible reaction mechanisms, aiding to the design of a more effective catalytic system. A broad substrate scope, the avoidance of toxic co–solvents and low catalyst loading still have to be realized with Ru–based catalysts, even if preliminary results are promising.

As a general statement, acceptorless dehydrogenation seems to be the main process involved even in more complex systems such as sugars and cellulose. Although very interesting results already show a possible role for finely tuned homogeneous catalysis in this field (at most for the importance to understand reaction mechanism at the moment), hydrogen production from these bio–derived substrates is still far from being adequate for large scale application. This means that there is still plenty of room to develop more active, stable and recyclable systems, following approaches previously described for simpler substrates (e.g. immobilization or tandem techniques) or designing new homogeneous systems on the base of already explored catalytic cycles.

3. Summary and Outlook

Hydrogen is deeply recognized as a suitable secondary energy feedstock. It could become sustainable if derived from green electrolysis or from biomass derived feedstocks efficiently transformed. As with the fossil derived hydrogen processes, catalysis plays a crucial role in order to develop new strategies for variously complex bio–derived compounds and mixtures. Main concerns arose from high oxygen contents in renewable crude materials which provide the more selectivity issues, the higher it is the intricacy of feedstock structures. Although heterogeneous catalysis still results more favourable, especially for low molecular weight substrates, homogeneous approaches can provide complementary advantages and have the prospective to solve some of the issues typical of classical processes. Indeed, if efficiency and recyclability of homogeneous catalysis (still the main drawbacks in the field) could be overcome, the milder reaction conditions could improve both energetic costs and overall selectivity. This latter being compulsory while employing complicated mixtures. Nevertheless, the tuning of molecular complexes in order to finely control several parameters, is deeper due to the directional previsions on inner and outer sphere cooperation by means of mechanistic investigation.

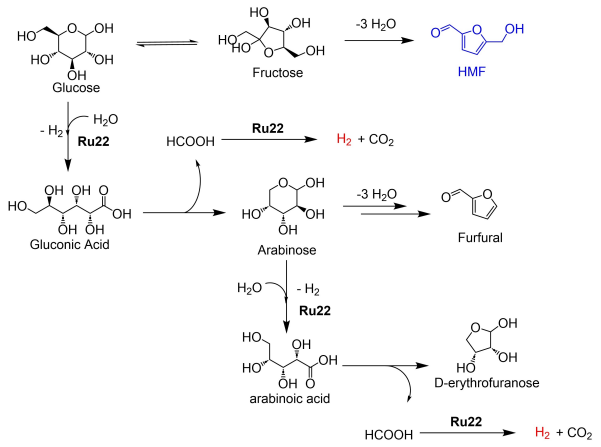

Scheme 24. Proposed mechanism of hydrogen production from glucose catalysed by **Ru 22** with the detected intermediates.[185]

In this paper the recent advances in development and application of molecular catalysis to pure hydrogen production have been described and commented. The majority of substrates under studies in the heterogeneous counterparts is nowadays subject of research for molecular driven application. The most reported is the work on hydrogen production from formic acid, followed by alcohol acceptorless dehydrogenation, with methanol still with a prominent role. Polyalcohols also allow for the reversible generation of hydrogen and are increasing the interests in production of valuable products accompanied by hydrogen production as a win–win perspective. Last but definitely not least, homogeneous catalysis is taking his first steps on production of hydrogen from variably functionalized sugars and cellulose. Independent reactivity, under reaction conditions required for hydrogen production of these substrates, takes the game to a higher level. Although molecular catalysis is still in its infancy in this field and up to date gave rise to low hydrogen production efficiency if compared to the potential content, the possibility to increase selectivity and to deeply understand main processes and side reactions vs conditions and catalyst role, makes these challenging approaches now prone to a better understanding and to the design of new and more efficient solutions.

As a general perspective, new knowledge within the field of molecular catalysed pure hydrogen production has been introduced within the last years research. To short summarize fine reactivity studies on easier substrates, such as formic acid, alcohols and polyols accompanied by DFT calculations, shed more light on metal–ligand cooperation. They indicate improvements from synergistic effects of additives or bi-catalytic systems able to lower or remove the necessity to use a base to activate the systems. On the other hand, the development of stable and recyclable immobilized molecular catalysts, especially when employing organometallic co–polymers, paves the way towards a new era for heterogenization of molecular catalysis. Often seriously affected by leaching and lower activity if compared to the homogeneous counterparts, it demonstrated in more than one example that can be a feasible way to be conducted with curiosity to better developments towards application.

A final remark is deserved to Earth–abundant metal molecular catalysts. Several examples of effective Fe and Mn based catalysts have been demonstrating that this is a path that needs to be further explored. It needs more efficiency, but

© 2024 The Author(s). ChemCatChem published by Wiley-VCH GmbH

18673899, 2024, 17, Downloaded from https://chemistry-europe.onlinelibrary.wiley.com/doi/10.1002/cctc.202400393 by CochraneItalia, Wiley Online Library on [25/03/2025]. See the Terms and Conditions (https://onlinelibrary.wiley.com/terms-and-conditions) on Wiley Online Library for rules of use; OA articles are governed by the applicable Creative Commons License

lower cost and higher sustainability of catalysts is becoming urgent in a circular economy point of view.

Still not really closed to bulk industrial application, homogeneous/heterogenized molecular catalysis seems to have acquired, in the last few years, some more talents in implementing stability and recyclability solutions and in reducing the number of required reactants in pure hydrogen production from simple substrates. More complex ones will require a little more time but the way is generally paved in the right direction.

Abbreviations

APR	Aqueous Phase Reforming
WGSR	Water Gas Shift Reaction
LOHC	Liquid Organic Hydrogen Carrier
FA	Formic Acid
DH	Dehydrogenation
FADH	FA Dehydrogenation
TOF	Turn Over Frequency
TON	Turn Over Number
DMSO	Dimethylsulphoxide
NHC	N-Heterocyclic Carbene
[BMIM][OAc]	1-butyl-3-methylimidazolium acetate
SLP	supported liquid phase
SILP	supported ionic liquid phase
PMO	Periodic Mesoporous Organosilica
EG	Ethylen glycol
DME	Dimethoxyethane
HEG	Hydroxyethyl Glycolate
1,2-PDO	1,2-propandiol
THF	tetrahydrofuran
DCM	Dichlorometane
$[Bu_4P][Me{-}P(OH)O_2]$	tetrabutylphosphonium methylphosphonate
HMF	5-hydroxymethylfurfural
NMP	N-methylpyrrolidone
AWS	Aldehyde Water Shift
DFT	density functional theory
[BMIM][TfO]	1-butyl-3-methylimidazolium trifluoromethanesulfonate.

Acknowledgements

We gratefully acknowledge the University of Bologna. Part of this work was financed by the European Union – NextGeneration EU through the Italian Ministry of University and Research under PNRR "Piano Nazionale di Ripresa e Resilienza" – Mission 4 "Istruzione e Ricerca" Component 2 "Dalla ricerca all'impresa", Investment 1.1, "Fondo per il Programma Nazionale di Ricerca e Progetti di Rilevante Interesse Nazionale (PRIN) – Piano Nazionale di Ripresa e Resilienza, addressed to Progetti di Ricerca di Rilevante Interesse Nazionale". D. D. n. 104 del 2/2/2022, Project title: Biomass–derived alcohols and polyols valorization and use by dehydrogenation/hydrogenation reactions promoted by bifunctional and proton–responsive homogeneous catalysts (ALCOVAL)", codice 20225 N5T5B – CUP J53D23008500006" AF acknowledges a research contract co–funded by European Union – PON Ricerca e Innovazione 2014–2020, art. 24, comma 3, lett. a), Legge 30 dicembre 2010, n. 240 e s.m.i. e del D. M. 10 agosto 2021 n. 1062. RM and MC acknowledge funding from "Agritech National Research Center": funding from the European Union Next–Generation EU (PIANO NAZIONALE DI RIPRESA E RESILIENZA (PNRR) – MISSIONE 4 COMPONENTE 2, INVESTIMENTO 1.4–D. D. 1032 17/06/2022, CN00000022)". JDM also acknowledges funding from European Commission, NextGenerationEU – Piano Nazionale di Ripresa e Resilienza (PNRR) – Ministero dell'Università e della Ricerca (MUR), (project number PE_00000021) Open Access publishing facilitated by Università degli Studi di Bologna, as part of the Wiley - CRUI-CARE agreement.

Conflict of Interests

The authors declare no conflict of interest.

Keywords: Hydrogen production · Aqueous Phase Reforming (APR) · alcohols · glucose · cellulose

[1] European Commission e Directorate General for Communication, "REPowerEU, joint European action for more affordable, secure and sustainable energy" *Publications Office of the European Union* **2022**.
[2] Mission Innovation, "Clean Hydrogen" can be found under https://explore.mission-innovation.net/mission/clean-hydrogen/, **2023** (accessed: 20/02/2024).
[3] US. Department of Energy, "Hydrogen Shot" can be found under https://www.energy.gov/eere/fuelcells/hydrogen-shot, 2023 (accessed: 20/02/2024).
[4] Green Hydrogen Organisation, "National Green Hydrogen Mission" can be found under https://gh2.org/countries/india#:~:text=Capacity%20and%20price,by%202030%20of%20electrolysis%20capacity, **2023** (accessed: 20/02/2024).
[5] International Energy Agency, "Hydrogen Industry Development Plan (2021–2035)" can be found under https://www.iea.org/policies/16977-hydrogen-industry-development-plan-2021-2035, **2023** (accessed: 20/02/2024).
[6] Hydrogen Council, "Hydrogen Insights 2023 December Update" can be found under https://hydrogencouncil.com/en/hydrogen-insights-2023-december-update/, **2023** (accessed: 20/02/2024).
[7] Y. Y. Tye, K. T. Lee, W. N. Wan Abdullah, C. P. Leh, *Renewable Sustainable Energy Rev.* **2016**, *60*, 155.
[8] A. Fasolini, R. Cucciniello, E. Paone, F. Mauriello, T. Tabanelli, *Catalysts* **2019**, *9*, 917.
[9] E. Pinto, W. N. Aggrey, P. Boakye, G. Amenuvor, Y. A. Sokama-Neuyam, M. K. Fokuo, H. Karimaie, K. Sarkodie, C. D. Adenutsi, S. Erzuah, M. Ama D Rockson, *Scientific African* **2022**, *15*, e01078.
[10] A. Galadima, A. Masudi, O. Muraza, *Microporous Mesoporous Mater.* **2022**, *336*, 111846.
[11] N. V. Gromov, T. B. Medvedeva, Y. A. Rodikova, M. N. Timofeeva, V. N. Panchenko, O. P. Taran, I. V. Kozhevnikov, V. N. Parmon, *Bioresour. Technol.* **2021**, *319*, 124122.
[12] P. A. Kamble, C. P. Vinod, V. K. Rathod, M. L. Kantam, *ChemCatChem* **2024**, e202301590.
[13] G. Galletti, P. Prete, S. Vanzini, R. Cucciniello, A. Fasolini, J. De Maron, F. Cavani, T. Tabanelli, *ACS Sustainable Chem. Eng.* **2022**, *10*, 10922.
[14] T. D. J. te Molder, S. R. A. Kersten, J. P. Lange, M. P. Ruiz, *Ind. Eng. Chem. Res.* **2021**, *60*, 7043.
[15] Y. Zhu, J. Yang, F. Mei, X. Li, C. Zhao, *Green Chem.* **2022**, *24*, 6450.
[16] S. Rajeswari, D. Baskaran, P. Saravanan, M. Rajasimman, N. Rajamohan, Y. Vasseghian, *Fuel* **2022**, *317*, 123448.
[17] D. A. Bulushev, J. R. H. Ross, *ChemSusChem* **2018**, *11*, 821.

© 2024 The Author(s). ChemCatChem published by Wiley-VCH GmbH

18673899, 2024, 17, Downloaded from https://chemistry-europe.onlinelibrary.wiley.com/doi/10.1002/cctc.202400393 by CochraneItalia, Wiley Online Library on [25/03/2025]. See the Terms and Conditions (https://onlinelibrary.wiley.com/terms-and-conditions) on Wiley Online Library for rules of use; OA articles are governed by the applicable Creative Commons License

[18] A. Malmusi, J. V. Ochoa, T. Tabanelli, F. Basile, C. Lucarelli, S. Agnoli, F. Carraro, G. Granozzi, F. Cavani, *Appl. Cat. A: Gen.* **2019**, *570*, 139.
[19] C. Antonetti, D. Licursi, S. Fulignati, G. Valentini, A. M. Raspolli Galletti, *Catalysts* **2016**, *6*, 196.
[20] C. Antonetti, A. M. Raspolli Galletti, D. Licursi, S. Fulignati, N. Di Fidio, F. Zanetti, A. Monti, T. Tabanelli, F. Cavani, *Catalysts* **2022**, *12*, 1189.
[21] A. Fasolini, D. Cespi, T. Tabanelli, R. Cucciniello, F. Cavani, *Catalysts* **2019**, *9*, 722.
[22] R. Davda, J. Shabaker, G. Huber, R. Cortright, J. Dumesic, *Appl. Catal. B* **2005**, *56*, 171.
[23] A. Fasolini, E. Lombardi, T. Tabanelli, F. Basile, *Nanomater.* **2021**, *11*, 1175.
[24] G. Huber, J. Dumesic, *Catal. Today* **2006**, *111*, 119.
[25] G. Huber, J. Shabaker, J. Dumesic, *Science* **2003**, *300*, 2075.
[26] J. Shabaker, R. Davda, G. Huber, R. Cortright, J. Dumesic, *J. Catal.* **2003**, *215*, 344.
[27] R. Cortroght, R. Davda, J. Dumesic, *Nature* **2002**, *418*, 964.
[28] G. Pipitone, G. Zoppi, R. Pirone, S. Bensaid, *Int. J. Hydrogen Energy* **2022**, *47*, 151.
[29] P. Vaidya, J. Lopez-Sanchez, *ChemistrySelect* **2017**, *2*, 6563.
[30] I. Coronado, M. Stekrova, M. Reinikainen, P. Simell, L. Lefferts, J. Lehtonen, *Int. J. Hydrogen Energy* **2016**, *41*, 11003.
[31] A. Joshi, P. Vaidya, *Int. J. Hydrogen Energy* **2024**, *49*, 117.
[32] G. Zoppi, G. Pipitone, R. Pirone, S. Bensaid, *Catal. Today* **2022**, *387*, 224.
[33] D. Grenoble, M. Estadt, D. Ollis, *J. Catal.* **1981**, *67*, 90.
[34] R. Davda, R. Alcala, J. Shabaker, G. Huber, R. Crtright, M. Mavrikakis, J. Dumesic, *Stud. Surf. Sci. Catal.* **2003**, *145*, 79.
[35] R. Davda, J. Shabaker, G. Huber, R. Crtright, J. Dumesic, *Appl. Catal. B* **2003**, *43*, 13.
[36] G. Samorjai, Y. Li, *Introduction to Surface Chemistry and Catalysis*, Wiley, **2010**, 1-784.
[37] G. Eggleston, J. Vercellotti, *J. Carbohydr. Chem.* **2008**, *19*, 1305.
[38] B. Kabyemela, T. Adschiri, R. Malaluan, K. Arai, *Ind. amp. Eng. Chem. Res.* **1997**, *36*, 1552.
[39] B. Kabyemela, T. Adschiri, R. Malaluan, K. Arai, *Ind. Eng. Chem. Res.* **1999**, *38*, 2888.
[40] J. Eppinger, K. W. Huang, *ACS Energy Lett.* **2017**, *2*, 188.
[41] P. G. Jessop, T. Ikariya, R. Noyori, *Chem. Rev.* **1995**, *95*, 259.
[42] M. Iguchi, Y. Himeda, Y. Manaka, K. Matsuoka, H. Kawanami, *ChemCatChem* **2016**, *8*, 886.
[43] F. Joó, *ChemSusChem* **2008**, *1*, 805.
[44] S. Enthaler, J. von Langermann, T. Schmidt, *Energy Environ. Sci.* **2010**, *3*, 1207.
[45] J. J. Baschuk, X. Li, *Int. J. Energy Res.* **2001**, *25*, 695.
[46] C. Guan, Y. Pan, T. Zhang, M. J. Ajitha, K. W. Huang, *Chem. Asian J.* **2020**, *15*, 937.
[47] L. Piccirilli, D. Lobo Justo Pinheiro, M. Nielsen, *Catalysts* **2020**, *10*, 773.
[48] J. Rana, S. T. Sahoo, P. Daw, *Tetrahedron* **2021**, *99*, 132473.
[49] M. Iglesias, F. J. Fernández-Alvarez, *Catalysts* **2021**, *11*, 1288.
[50] N. Onishi, R. Kanega, H. Kawanami, Y. Himeda, *Molecules* **2022**, *27*, 455.
[51] A. Kumar, P. Daw, D. Milstein, *Chem. Rev.* **2022**, *122*, 385.
[52] A. Wang, P. He, J. Wu, N. Chen, C. Pan, E. Shi, H. Jia, T. Hu, K. He, Q. Cai, R. Shen, *Energy Fuels* **2023**, *37*, 17075.
[53] S. Kushwaha, J. Parthiban, S. K. Singh, *ACS Omega* **2023**, *8*, 38773.
[54] S. Zhai, S. Jiang, C. Liu, Z. Li, T. Yu, L. Sun, G. Ren, W. Deng, *J. Phys. Chem. Lett.* **2022**, *13*, 8586.
[55] I. Dutta, S. Chatterjee, H. Cheng, R. K. Parsapur, Z. Liu, Z. Li, E. Ye, H. Kawanami, J. S. C. Low, Z. Lai, X. J. Loh, K.-W. Huang, *Adv. Energy Mater.* **2022**, *12*, 2103799.
[56] S. Patra, B. Maji, H. Kawanami, Y. Himeda, *RSC Sustainability* **2023**, *1*, 1655.
[57] M. Solakidou, A. Gemenetzi, G. Koutsikou, M. Theodorakopoulos, Y. Deligiannakis, M. Louloudi, *Energies* **2023**, *16*, 1723.
[58] R. S. Coffey, *Chem. Commun.* **1967**, 923.
[59] J. H. Barnard, C. Wang, N. G. Berry, J. Xiao, *Chem. Sci.* **2013**, *4*, 1234.
[60] W.-H. Wang, M. Z. Ertem, S. Xu, N. Onishi, Y. Manaka, Y. Suna, H. Kambayashi, J. T. Muckerman, E. Fujita, Y. Himeda, *ACS Catal.* **2015**, *5*, 5496.
[61] Z. Wang, S.-M. Lu, J. Li, J. Wang, C. Li, *Chem. Eur. J.* **2015**, *21*, 12592.
[62] J. J. A. Celaje, Z. Lu, E. A. Kedzie, N. J. Terrile, J. N. Lo, T. J. Williams, *Nat. Commun.* **2016**, *7*, 11308.
[63] N. Onishi, M. Z. Ertem, S. Xu, A. Tsurusaki, Y. Manaka, J. T. Muckerman, E. Fujita, Y. Himeda, *Catal. Sci. Technol.* **2016**, *6*, 988.
[64] H. Kawanami, M. Iguchi, Y. Himeda, *Inorg. Chem.* **2020**, *59*, 4191.
[65] W.-H. Wang, H. Wang, Y. Yang, X. Lai, Y. Li, J. Wang, Y. Himeda, M. Bao, *ChemSusChem* **2020**, *13*, 5015.
[66] S. Cheng, Z. Lang, J. Du, Z. Du, Y. Li, H. Tan, Y. Li, *J. Catal.* **2022**, *413*, 119.
[67] L. Guo, Z. Li, M. Cordier, R. Marchal, B. Le Guennic, C. Fischmeister, *ACS Catal.* **2023**, *13*, 13626.
[68] H. Liu, W.-H. Wang, H. Xiong, A. Nijamudheen, M. Z. Erdem, M. Wang, L. Duan, *Inorg. Chem.* **2021**, *60*, 3410.
[69] R. Kanega, N. Onishi, L. Wang, K. Murata, T. J. Muckerman, E. Fujita, Y. Himeda, *Chem. Eur. J.* **2018**, *24*, 18389.
[70] G. Menendez Rodriguez, C. Domestici, A. Bucci, M. Valentini, C. Zuccaccia, A. Macchioni, *Eur. J. Inorg. Chem.* **2018**, 2247.
[71] R. Kanega, M. Z. Ertem, N. Onishi, D. J. Szalda, E. Fujita, Y. Himeda, *Organometallics* **2020**, *39*, 1519.
[72] J. Guo, C. Yin, M. Li, D. Zhong, Y. Zhang, X. Li, Y. Wang, H. Yao, T. Qi, *Asian J. Org. Chem.* **2022**, *11*, e202100562.
[73] J. Guo, M. Li, C. Yin, X. Li, Y. Wang, J. Yuan, T. Qi, *Dalton Trans.* **2023**, *52*, 4856.
[74] J. Guo, M. Li, C. Yin, D. Zhong, Y. Zhang, X. Li, Y. Wang, J. Yuan, H. Xie, T. Qi, *Inorg. Chem.* **2023**, *62*, 18982.
[75] N. Lentz, M. Albrecht, *ACS Catal.* **2022**, *12*, 12627.
[76] B. Maji, A. Kumar, A. Bhattacherya, J. K. Bera, J. Choudhury, *Organometallics* **2022**, *41*, 3589.
[77] S. Patra, S. K. Singh, *Inorg. Chem.* **2020**, *59*, 4234.
[78] S. Kushwaha, J. Parthiban, S. K. Singh, *Organometallics* **2023**, *42*, 3066.
[79] S. Kushwaha, M. K. Awasthi, A. Das, B. Pathak, S. K. Singh, *Inorg. Chem.* **2023**, *62*, 8080.
[80] S. Patra, H. Deka, S. K. Singh, *Inorg. Chem.* **2021**, *60*, 14275.
[81] S. Kar, M. Rauch, G. Leitus, Y. Ben-David, D. Milstein, *Nat. Catal.* **2021**, *4*, 193.
[82] Q. Wang, Y. Xia, F. Cheng, Z. Chen, Y. Wang, X. Zhou, L. Qin, Z. Zheng, *Chin. J. Chem.* **2021**, *39*, 2201.
[83] P. Knörr, N. Lentz, M. Albrecht, *Catal. Sci. Technol.* **2023**, *13*, 5625.
[84] R. Verron, E. Puig, P. Sutra, A. Igau, C. Fischmeister, *ACS Catal.* **2023**, *13*, 5787.
[85] L. Piccirilli, B. Rabell, R. Padilla, A. Riisager, S. Das, M. Nielsen, *J. Am. Chem. Soc.* **2023**, *145*, 5655.
[86] A. Boddien, F. Gärtner, R. Jackstell, H. Junge, A. Spannenberg, W. Baumann, R. Ludwig, M. Beller, *Angew. Chem. Int. Ed.* **2010**, *49*, 8993.
[87] A. Boddien, B. Loges, F. Gärtner, C. Torborg, K. Fumino, H. Junge, R. Ludwig, M. Beller, *J. Am. Chem. Soc.* **2010**, *132*, 8924.
[88] A. Boddien, D. Mellmann, F. Gärtner, R. Jackstell, H. Junge, P. J. Dyson, G. Laurenczy, R. Ludwig, M. Beller, *Science* **2011**, *333*, 1733.
[89] T. Zell, B. Butschke, Y. Ben-David, D. Milstein, *Chem. Eur. J.* **2013**, *19*, 8068.
[90] E. A. Bielinski, P. O. Lagaditis, Y. Zhang, B. Q. Mercado, C. Würtele, W. H. Bernskoetter, N. Hazari, S. Schneider, *J. Am. Chem. Soc.* **2014**, *136*, 10234.
[91] F. Bertini, I. Mellone, A. Ienco, M. Peruzzini, L. Gonsalvi, *ACS Catal.* **2015**, *5*, 1254.
[92] I. Mellone, N. Gorgas, F. Bertini, M. Peruzzini, K. Kirchner, L. Gonsalvi, *Organometallics* **2016**, *35*, 3344.
[93] M. Montandon-Clerc, A. F. Dalebrook, G. Laurenczy, *J. Catal.* **2016**, *343*, 62.
[94] E. Balaraman, A. Nandakumar, G. Jaiswalab, M. K. Sahoo, *Catal. Sci. Technol.* **2017**, *7*, 3177.
[95] J. B. Curley, N. E. Smith, W. H. Bernskoetter, N. Hazari, B. Q. Mercado, *Organometallics* **2018**, *37*, 3846.
[96] A. M. Tondreau, J. M. Boncella, *Organometallics* **2016**, *35*, 2049.
[97] N. H. Anderson, J. Boncella, A. M. Tondreau, *Chem. Eur. J.* **2019**, *25*, 10557.
[98] M. Onishi, *J. Mol. Catal.* **1993**, *80*, 145.
[99] W. Zhou, Z. Wei, A. Spannenberg, H. Jiao, K. Junge, H. Junge, M. Beller, *Chem. Eur. J.* **2019**, *25*, 8459.
[100] S. Enthaler, A. Brück, A. Kammer, H. Junge, E. Irran, S. Gülak, *ChemCatChem* **2015**, *7*, 65.
[101] M. C. Neary, G. Parkin, *Dalton Trans.* **2016**, *45*, 14645.
[102] N. Scotti, R. Psaro, N. Ravasio, F. Zaccheria, *RSC Adv.* **2014**, *4*, 61514.
[103] A. Correa, M. Cascella, N. Scotti, F. Zaccheria, N. Ravasio, R. Psaro, *Inorg. Chim. Acta* **2018**, *470*, 290.
[104] T. Nakajima, Y. Kamiryo, M. Kishimoto, K. Imai, K. Nakamae, Y. Ura, T. Tanase, *J. Am. Chem. Soc.* **2019**, *141*, 8732.
[105] K. Phung, P. Thuéry, J.-C. Berthet, T. Cantat, *Organometallics* **2023**, *42*, 3357.

© 2024 The Author(s). ChemCatChem published by Wiley-VCH GmbH

18673899, 2024, 17, Downloaded from https://chemistry-europe.onlinelibrary.wiley.com/doi/10.1002/cctc.202400393 by CochraneItalia, Wiley Online Library on [25/03/2025]. See the Terms and Conditions (https://onlinelibrary.wiley.com/terms-and-conditions) on Wiley Online Library for rules of use; OA articles are governed by the applicable Creative Commons License

[106] A. Mishra, D. Srivastava, D. Raj, N. Patra, S. K. Padhi, *Dalton Trans.* **2024**, *53*, 1209.
[107] J. B. Curley, W. H. Bernskoetter, N. Hazari, *ChemCatChem* **2020**, *12*, 1934.
[108] J. B. Curley, N. E. Smith, W. H. Bernskoetter, M. Z. Ertem, N. Hazari, B. Q. Mercado, T. M. Townsend, X. Wang, *ACS Catal.* **2021**, *11*, 10631.
[109] J. B. Curley, T. M. Townsend, W. H. Bernskoetter, N. Hazari, B. Q. Mercado, *Organometallics* **2022**, *41*, 301.
[110] A. Léval, A. Agapova, C. Steinlechner, E. Alberico, H. Junge, M. Beller, *Green Chem.* **2020**, *22*, 913.
[111] A. Léval, H. Junge, M. Beller, *Catal. Sci. Technol.* **2020**, *10*, 3931.
[112] D. Wei, R. Sang, P. Sponholz, H. Junge, M. Beller, *Nat. Energy* **2022**, *7*, 438.
[113] D. Wei, X. Shi, P. Sponholz, H. Junge, M. Beller, *ACS Cent. Sci.* **2022**, *8*, 1457.
[114] N. Johnee Britto, M. Jaccob, *Inorg. Chem.* **2021**, *60*, 11038.
[115] I. Dutta, N. A. Alobaid, F. L. Menicucci, P. Chakraborty, C. Guan, D. Han, K. W. Huang, *Int. J. Hydrogen Energy* **2023**, *48*, 26559.
[116] N. Lentz, A. Aloisi, P. Thuéry, E. Nicola, T. Cantat, *Organometallics* **2021**, *40*, 565.
[117] C.-P. Tsai, C.-Y. Chen, Y.-L. Lin, J.-C. Lan, M.-L. Tsai, *Inorg. Chem.* **2024**, *63*, 1759.
[118] A. Friedrich, S. Schneider, *ChemCatChem* **2009**, *1*, 72.
[119] V. Yadav, G. Sivakumar, V. Gupta, E. Balaraman, *ACS Catal.* **2021**, *11*, 14712.
[120] E. Alberico, M. Nielsen, *Chem. Commun.* **2015**, *51*, 6714.
[121] J. Kothandaraman, S. Kar, A. Goeppert, R. Sen, G. K. S. Prakash, *Top. Catal.* **2018**, *61*, 542.
[122] K. Sordakis, C. Tang, L. K. Vogt, H. Junge, P. J. Dyson, M. Beller, G. Laurenczy, *Chem. Rev.* **2018**, *118*, 372.
[123] N. Onishi, G. Laurenczy, M. Beller, Y. Himeda, *Coord. Chem. Rev.* **2018**, *373*, 317.
[124] M. Trincado, D. Banerjee, H. Grützmacher, *Chem. Commun.* **2015**, *51*, 6714.
[125] C. Gunanathan, D. Milstein, *Science* **2013**, *341*, 1229712.
[126] M. Nielsen, E. Alberico, W. Baumann, H. J. Drexler, H. Junge, S. Gladiali, M. Beller, *Nature* **2013**, *495*, 85.
[127] V. Strobel, J. J. Schuster, A. S. Braeuer, L. K. Vogt, H. Junge, M. Haumann, *React. Chem. Eng.* **2017**, *2*, 390.
[128] Y. Y. Jiang, Z. Y. Xu, H. Z. Yu, Y. Fu, *Sci. China Chem.* **2016**, *59*, 724.
[129] M. Lei, Y. Pan, X. Ma, *Eur. J. Inorg. Chem.* **2015**, 794.
[130] X. Yang, *ACS Catal.* **2014**, *4*, 1129.
[131] E. Alberico, A. J. J. Lennox, L. K. Vogt, H. Jiao, W. Baumann, H. J. Drexler, M. Nielsen, A. Spannenberg, M. P. Checinski, H. Junge, M. Beller, *J. Am. Chem. Soc.* **2016**, *138*, 14890.
[132] R. E. Rodríguez-Lugo, M. Trincado, M. Vogt, F. Tewes, G. Santiso-Quinones, H. Grützmacher, *Nat. Chem.* **2013**, *5*, 342.
[133] Y. Jing, X. Chen, X. Yang, *J. Organomet. Chem.* **2016**, *820*, 55.
[134] H. Li, M. B. Hall, *J. Am. Chem. Soc.* **2015**, *137*, 12330.
[135] V. Sinha, M. Trincado, H. Grützmacher, B. De Bruin, *J. Am. Chem. Soc.* **2018**, *140*, 13103.
[136] A. Monney, E. Barsch, P. Sponholz, H. Junge, R. Ludwig, M. Beller, *Chem. Commun.* **2014**, *50*, 707.
[137] P. Hu, Y. Diskin-Posner, Y. Ben-David, D. Milstein, *ACS Catal.* **2014**, *4*, 2649.
[138] F. F. van de Watering, M. Lutz, W. I. Dzik, B. de Bruin, J. N. H. Reek, *ChemCatChem* **2016**, *8*, 2752.
[139] F. J. de Zwart, V. Sinha, M. Trincado, H. Grützmacher, B. de Bruin, *Dalton Trans.* **2022**, *51*, 3019.
[140] V. Sinha, N. Govindarajan, B. de Bruin, E. Jan Meijer, *ACS Catal.* **2018**, *8*, 6908.
[141] J. Campos, L. S. Sharninghausen, M. G. Manas, R. H. Crabtree, *Inorg. Chem.* **2015**, *54*, 5079.
[142] K. Fujita, R. Kawahara, T. Aikawa, R. Yamaguchi, *Angew. Chem. Int. Ed.* **2015**, *54*, 9057.
[143] W.-H. Wang, J. F. Hull, J. T. Muckerman, E. Fujita, Y. Himeda, *Energy Environ. Sci.* **2012**, *5*, 7923.
[144] Y. Suna, M. Z. Ertem, W.-H. Wang, H. Kambayashi, Y. Manaka, J. T. Muckerman, E. Fujita, Y. Himeda, *Organometallics* **2014**, *33*, 6519.
[145] Y. Li, P. Sponholz, M. Nielsen, H. Junge, M. Beller, *ChemSusChem* **2015**, *8*, 804.
[146] D. Morton, D. J. Cole-Hamilton, *J. Chem. Soc. Chem. Commun.* **1987**, 248.
[147] Y. L. Zhan, Y. B. Shen, S. P. Li, B. H. Yue, X. C. Zhou, *Chin. Chem. Lett.* **2017**, *28*, 1353.
[148] J. Rana, S. Tanaya Sahoo, P. Daw, *Tetrahedron* **2021**, *99*, 132473.
[149] E. Alberico, P. Sponholz, C. Cordes, M. Nielsen, H. J. Drexler, W. Baumann, H. Junge, M. Beller, *Angew. Chem. Int. Ed.* **2013**, *52*, 14162.
[150] M. Andérez-Fernández, L. K. Vogt, S. Fischer, W. Zhou, H. Jiao, M. Garbe, S. Elangovan, K. Junge, H. Junge, R. Ludwig, M. Beller, *Angew. Chem. Int. Ed.* **2017**, *56*, 559.
[151] E. A. Bielinski, M. Förster, Y. Zhang, W. H. Bernskoetter, N. Hazari, M. C. Holthausen, *ACS Catal.* **2015**, *5*, 2404.
[152] A. Agapova, H. Junge, M. Beller, *Chem. Eur. J.* **2019**, *25*, 9345.
[153] Y. Shen, Y. Zhan, S. Li, F. Ning, Y. Du, Y. Huang, T. He, X. Zhou, *Chem. Sci.* **2017**, *8*, 7498.
[154] Y. Shen, Y. Zhan, S. Li, F. Ning, Y. Du, Y. Huang, T. He, X. Zhou, *ChemSusChem* **2018**, *11*, 864.
[155] J. Luo, S. Kar, M. Rauch, M. Montag, Y. Ben-David, D. Milstein, *J. Am. Chem. Soc.* **2021**, *143*, 17284.
[156] C. H. Schwarz, A. Agapova, H. Junge, M. Haumanna, *Catal. Today* **2020**, *342*, 178.
[157] S. Yamaguchi, Y. Maegawa, K. Fujita, S. Inagaki, *ChemSusChem* **2021**, *14*, 1074.
[158] P. Sponholz, D. Mellmann, C. Cordes, P. G. Alsabeh, B. Li, Y. Li, M. Nielsen, H. Junge, P. Dixneuf, M. Beller, *ChemSusChem* **2014**, *7*, 2419.
[159] M. Nielsen, A. Kammer, D. Cozzula, H. Junge, S. Gladiali, M. Beller, *Angew. Chem. Int. Ed.* **2011**, *50*, 9593.
[160] M. Nielsen, H. Junge, A. Kammer, M. Beller, *Angew. Chem. Int. Ed.* **2012**, *51*, 5711.
[161] M. Trincado, D. Banerjeea, H. Grutzmacherab, *Energy Environ. Sci.* **2014**, *7*, 2464.
[162] C. Ma, L. Qin, Z. Zheng, *J. Organomet. Chem.* **2024**, *1004*, 122950.
[163] M. Onoda, Y. Nagano, K. Fujita, *Int. J. Hydrogen Energy* **2019**, *44*, 28514.
[164] H. Yue, Y. Zhao, X. Ma, J. Gong, *Chem. Soc. Rev.* **2012**, *41*, 4218.
[165] M. Trincado, K. Kühlein, H. Grützmacher, *Chem. Eur. J.* **2011**, *17*, 11905.
[166] T. Van Haasterecht, T. W. van Deelen, K. P. de Jong, J. H. Bitter, *Catal. Sci. Technol.* **2014**, *4*, 2353.
[167] Y. Zhan, W. Hou, G. Li, Y. Shen, Y. Zhang, Y. Tang, *ACS Sustainable Chem. Eng.* **2019**, *7*, 17559.
[168] A. Wang, T. Zhang, T. Acc, *Chem. Res.* **2013**, *46*, 1377.
[169] Y. Q. Zou, N. von Wolff, A. Anaby, Y. Xie, D. Milstein, *Nat. Catal.* **2019**, *2*, 415, and References therein.
[170] Y. -Qu Zou, N. von Wolff, M. Rauch, M. Feller, Q.-Q. Zhou, A. Anaby, Y. Diskin-Posner, L. J. W. Shimon, L. Avram, Y. Ben-David, D. Milstein, *Chem. Eur. J.* **2021**, *27*, 4715.
[171] Glycolic Acid Market–Forecasts from 2018 to 2023 can be found under https://www.researchandmarkets.com/reports/4542547/glycolic-acid-market-forecastsfrom-2018-to-2023, **2023** (accessed: 20/02/2024).
[172] S. D. Barnicki, R. T. Hembre, S. N. Falling, M. E. Janka, K. M. Moran, Patent, US-B2 8703999, **2014**.
[173] L. Prager, P. Dowideit, H. Langguth, H.-P. Schuchmann, C. von Sonntag, *J. Chem. Soc.-Perkin Trans.* **2001**, *2* 1641.
[174] D. Roberts, D. J. Watson, J. Swinney, patent WO-A1 2018/051115, **2018**.
[175] S. T. Sahoo, A. Mohanty, R. Sharma, P. Daw, *Dalton Trans.* **2023**, *52*, 15343.
[176] S. Waiba, M. Maiti, B. Maji, *ACS Catal.* **2022**, *12*, 3995.
[177] M. T. Azizan, A. Aqsha, M. Ameen, A. Syuhada, H. Klaus, S. Z. Abidin, F. Sher, *Biomass Convers. Biorefin.* **2023**, *13*, 8441.
[178] Y. Li, M. Nielsen, B. Li, P. H. Dixneuf, H. Junge, M. Beller, *Green Chem.* **2015**, *17*, 193.
[179] M. G. Manas, J. Campos, L. S. Sharninghausen, E. Lin, R. H. Crabtree, *Green Chem.* **2015**, *17*, 594.
[180] J. Wu, L. Shen, S. Duan, Z.-N. Chen, Q. Zheng, Y. Liu, Z. Sun, J. H. Clark, X. Xu, T. Tu, *Angew. Chem. Int. Ed.* **2020**, *59*, 13871.
[181] S. T. Sahoo, A. Mohanty, R. Sharma, S. R. Rout, R. Dandela, P. Daw, *Organometallics* **2023**, *42*, 745.
[182] Y.-J. Cheong, K. Sung, J.-A. Kim, Y. K. Kim, H.-Y. Jang, *Eur. J. Inorg. Chem.* **2020**, 4064.
[183] A. N. Hellman, N. A. Torquato, M. E. Foster, C. Dun, J. E. Reynolds, C. J. Yu, A. D. Tran, M. Shivanna, G. Frances, H. Garcia, J. Yang, Y. Chen, J. Su, J. J. Urban, M. D. Allendorf, V. Stavila, *ACS Appl. Energ. Mater.* **2023**, *6*, 7353.
[184] A. Mollar-Cuni, J. P. Byrne, P. Borja, C. Vicent, M. Albrecht, J. A. Mata, *ChemCatChem* **2020**, *12*, 3746.
[185] A. Messori, G. Martelli, A. Piazzi, F. Basile, J. De Maron, A. Fasolini, R. Mazzoni, *ChemPlusChem* **2023**, *88*, e202300357.
[186] N. Taccardi, D. Assenbaum, M. E. M. Berger, A. Bösmann, F. Enzenberger, R. Wölfel, S. Neuendorf, V. Goeke, N. Schödel, H.-J. Maass, H. Kistenmacher, P. Wasserscheid, *Green Chem.* **2010**, *12*, 1150.

© 2024 The Author(s). ChemCatChem published by Wiley-VCH GmbH

18673899, 2024, 17, Downloaded from https://chemistry-europe.onlinelibrary.wiley.com/doi/10.1002/cctc.202400393 by CochraneItalia, Wiley Online Library on [25/03/2025]. See the Terms and Conditions (https://onlinelibrary.wiley.com/terms-and-conditions) on Wiley Online Library for rules of use; OA articles are governed by the applicable Creative Commons License

[187] Y. Zhan, Y. Shen, S. Li, B. Yue, X. Zhou, *Chem. Commun.* **2017**, *53*, 4230.
[188] K–I. Fujita, T. Inoue, T. Tanaka, J. Jeong, S. Furukawa, R. Yamaguchi, *Catalysts* **2021**, *11*, 891.
[189] G. Toyooka, T. Tanaka, K. Kitayama, N. Kobayashi, T. Watanabe, K–I. Fujita, *Catal. Sci. Technol.* **2021**, *11*, 2273.
[190] H. Junge, B. Loges, M. Beller, *Chem. Commun.* **2007**, 522.
[191] P. Zhang, Y.-J. Guo, J. Chen, Y.-R. Zhao, J. Chang, H. Junge, M. Beller, Y. Li, *Nat. Catal.* **2018**, *1*, 332.
[192] P. Borja, C. Vicent, M. Baya, H. García, J. A. Mata, *Green Chem.* **2018**, *20*, 4094.
[193] B. L. Conley, M. K. Pennington-Boggio, E. Boz, T. J. Williams, *Chem. Rev.* **2010**, *110*, 2294.
[194] R. Mazzoni, C. Cesari, V. Zanotti, C. Lucarelli, T. Tabanelli, F. Puzzo, F. Passarini, E. Neri, G. Marani, R. Prati, F. Viganò, A. Conversano, F. Cavani, *ACS Sustainable Chem. Eng.* **2019**, *7*, 224.
[195] C. Cristiana, A. Gagliardi, A. Messori, N. Monti, V. Zanotti, S. Zacchini, I. Rivalta, F. Calcagno, C. Lucarelli, T. Tabanelli, F. Cavani, R. Mazzoni, *J. Catal.* **2022**, *405*, 47.
[196] A. Messori, A. Gagliardi, C. Cesari, F. Calcagno, T. Tabanelli, F. Cavani, R. Mazzoni, *Catal. Today* **2023**, *423*, 114003.
[197] C. Cesari, A. Cingolani, M. Teti, A. Messori, S. Zacchini, V. Zanotti, R. Mazzoni, *Eur. J. Inorg. Chem.* **2020**, 1114.
[198] T. Pasini, G. Solinas, V. Zanotti, S. Albonetti, F. Cavani, A. Vaccari, A. Mazzanti, S. Ranieri, R. Mazzoni, *Dalton Trans.* **2014**, *43*, 10224.
[199] C. Cesari, R. Mazzoni, E. Matteucci, A. Baschieri, L. Sambri, M. Mella, A. Tagliabue, F. L. Basile, C. Lucarelli, *Organometallics* **2019**, *38*, 1041.
[200] C. Cesari, A. Cingolani, C. Parise, S. Zacchini, V. Zanotti, M. C. Cassani, R. Mazzoni, *RSC Adv.* **2015**, *5*, 94707.
[201] C. Cesari, R. Mazzoni, H. Muller-Bunz, M. Albrecht, *J. Organomet. Chem.* **2015**, *793*, 256.
[202] A. S. Phearman, J. M. Moore, D. D. Bhagwandin, J. M. Goldberg, D. M. Heinekey, K. I. Goldberg, *Green Chem.* **2021**, *23*, 1609.

Manuscript received: February 27, 2024
Revised manuscript received: April 8, 2024
Accepted manuscript online: April 10, 2024
Version of record online: May 6, 2024

[Correction added on 27 December 2024, after first online publication: The copyright line was changed.].

© 2024 The Author(s). ChemCatChem published by Wiley-VCH GmbH

18673899, 2024, 17, Downloaded from https://chemistry-europe.onlinelibrary.wiley.com/doi/10.1002/cctc.202400393 by CochraneItalia, Wiley Online Library on [25/03/2025]. See the Terms and Conditions (https://onlinelibrary.wiley.com/terms-and-conditions) on Wiley Online Library for rules of use; OA articles are governed by the applicable Creative Commons License